

Isolation and Analysis of *Arabidopsis* Mutants
with Altered Leaf Thickness or Leaf Length

Noriyuki N. Narita

Doctor of Philosophy

2004

Department of Molecular Biomechanics
School of Life Science
The Graduate University for Advanced Studies

TABLE OF CONTENTS

GENERAL INTRODUCTION	1
CHAPTER I	
Overexpression of a Novel Small Peptide ROTUNDIFOLIA4 Decreases Cell Proliferation and Alters Leaf Shape in <i>Arabidopsis thaliana</i> .	
1 Introduction	3
2 Materials and Methods	5
3 Results	10
4 Discussion	16
CHAPTER II	
Development of Leaf Thickness Measurement Instrument and Anatomical Characterization of <i>Arabidopsis</i> Thick-leaf Mutant N692.	
1 Introduction	29
2 Materials and Methods	32
3 Results	33
4 Discussion	36
CONCLUSION	44
ACKNOWLEDGMENT	45
REFERENCES	46

GENERAL INTRODUCTION

Diversity in the architecture of vascular plants is established by combination of morphogenesis of leaf, stem and roots arising from meristems. Stems and roots make the primary and higher order axes by branching. Thus, the pattern of branching is a mechanism underlying the determination of overall plant shape. In contrast, leaf is a lateral organ and has an essentially planar shape. Therefore the diversity in leaf shape should be created by a fundamentally different mechanism(s) from those employed in stems and roots. In addition, leaf is another major determinant of whole plant shape since most aerial parts of a plant is covered with leaves. Within a given species, the shape of leaves could also be different according to the node number as well as in response to environmental conditions. Thus, intrinsic developmental programs are coordinated with external stimuli, enabling highly plastic development. Moreover, flowers are mainly modified leaf organs, so the morphogenesis of floral organs could be understood through leaf morphogenesis.

The diversity found in leaf shape reflects the evolutionary history and adaptation of currently existing plant species. Leaves are the primary organs for photosynthesis and plants that have adapted in a particular ecological niche should be able to survive by modifying leaf shape. Therefore, understandings of mechanisms of leaf morphogenesis are important for the elucidation of general plant morphogenesis as well as evolution and adaptation of plants.

Since leaves have three-dimensional formulation, it is thought that the mechanisms each controls growth and development along length, width or height direction would be important for leaf morphogenesis. This simplified idea seems helpful to dissect leaf morphogenesis into several elemental pathways. A number of mutants displaying disorganized leaf morphogenesis are often difficult to interpret how the normal gene function contributes to the developmental program of leaf shape control. Therefore, mutants with any specific defects in these axis-dependent mechanisms will provide fundamental knowledge about the leaf morphogenesis.

Several *Arabidopsis* mutants were isolated based on this idea in our laboratory. For example, leaves of

rotundifolia3-1 (rot3-1) are shortened specifically along length direction (Tsuge et al., 1996; Kim et al., 1998b). The cause of short-leaf phenotype is that cell shape is shortened along the leaf-length direction. The molecular genetic analysis revealed that *rot3-1* has a defect in the CYP90C1 that is involved in brassinosteroid biosynthesis pathway (Kim et al., 1998b, in press). However, it had not been known whether control of leaf length is exclusively mediated by cell expansion. Therefore I focused on another important process of morphogenesis, namely cell proliferation. Screening of T-DNA activation lines of *Arabidopsis thaliana* led to the isolation of a novel short-leaf mutant, *rot4-1D*. Leaves of this mutant have fewer cells than wild type specifically along the leaf-length direction. The results of detailed investigation are described in chapter I.

With respect to mutants that have a defect in the control of leaf width, *angustifolia-1 (an-1)* has been isolated (Tsuge et al., 1996). *an-1* has a defect in the polar expansion of cells like *rot3-1*, but the leaf cells are narrower and thicker than wild type (Tsuge et al., 1996). In *an-1* mutants, the abnormal orientation of the cortical microtubules was also found (Kim et al., 2002). Since orientation of cortical microtubule is important for the anisotropic cell expansion (Cyr, 1994; Shibaoka, 1994), the appropriate organization of cortical microtubule may be important for the determination of leaf width and thickness. However molecular function of AN is not well understood except that it is a homolog of transcriptional corepressor CtBP (Kim et al., 2002; Folkers et al., 2002; Cho et al., unpublished). In another narrow leaf mutant *an3*, the leaf width decreases due to the poor cell proliferation activity during the leaf blade expansion, and does not increase the leaf thickness (Horiguchi et al., unpublished).

As mentioned above, at present, isolation of mutants that have a specific defect in leaf thickness has been not reported. For the elucidation of the basic programs of leaf morphogenesis, I thought that identification of factors that specifically regulate leaf thickness is necessary. However, this has been hampered by the complicated procedure for the determination of leaf thickness. Therefore, I started the development of simple measurement system for the leaf thickness followed by the isolation of mutant with altered leaf thickness. The concept and usefulness of this system are described in chapter II. I believe that my results in this thesis should to better understandings of leaf-length and -thickness control.

CHAPTER I

Overexpression of a Novel Small Peptide ROTUNDIFOLIA4 Decreases Cell Proliferation and Alters Leaf Shape in *Arabidopsis thaliana*.

1 Introduction

Plant leaves exhibit great diversity in shape and size among different species. To understand the molecular basis of such morphological diversity, it is essential to reveal basic processes of leaf development. Since leaves of *Arabidopsis thaliana* are simple in shape, it is useful to understand how common developmental properties of leaf organ, such as dorsoventrality (Eshed et al., 2001; Kerstetter et al., 2001; McConnell et al., 2001; Sawa et al., 1999; Siegfried et al., 1999) and symmetry (Byrne et al., 2002; Iwakawa et al., 2002; Semiarti et al., 2001; Sun et al., 2002) are established (reviewed in Tsukaya, 2002).

Cell division and expansion are two major factors that influence organ shapes. Many mutants defective in cell expansion processes, including cell wall biosynthesis and modification (Cho and Cosgrove, 2000; Nicol et al., 1998), turgor generation (Dennison et al., 2001; Elumalai et al., 2002), endoreduplication (Sugimoto-Shirasu et al., 2002; reviewed in Sugimoto-Shirasu and Roberts, 2003) as well as hormone biogenesis and perception have been characterized (for review, see Tsukaya, 2003). In addition, transgenic plants, in which expression of core cell cycle genes such as CDKA;1 (Hemerly et al., 1995), CYCD3;1 (Dewitte et al., 2003), CDK inhibitors (De Veylder et al., 2001; Wang et al., 2000), E2F and DP (De Veylder et al., 2002) was manipulated, have been described. Many of these plants produced small leaves due to the inhibition of cell expansion, cell proliferation or cell differentiation. However, the relationship between the polar development of leaves and cell division and expansion is largely unknown.

To reveal the mechanisms of two-dimensional polar leaf development, Tsukaya and coworkers have screened for leaf-shape mutants with a specific alteration in either the length or width of leaf blade, and

have characterized two classes of mutants, namely *angustifolia* (*an*) and *rotundifolia* (*rot*). In leaves of *an* and *rot3*, cell size is reduced mainly in the leaf width- and leaf length directions, respectively (Tsuge et al., 1996). The *AN* and *ROT3* genes were found to encode a homolog of the transcription co-repressor, CtBP and a member of the cytochrome P450 family CYP90C1, potentially involved in brassinosteroid biosynthesis, respectively (Kim et al., 1998b, 1999, 2002). These results demonstrated that distinct mechanisms are involved in the control of leaf cell expansion in the leaf-length and -width directions. In contrast, control of cell division orientation during leaf development is poorly characterized. Mutants with reduced leaf cell proliferation such as *aintegumenta* (*ant*), *struwwelpeter* (*swp*), *pointed first leaf2* (*pfl2*) and *grf interacting factor1* exhibit narrow-leaf phenotypes (Autran et al., 2002; Ito et al., 2000; Mizukami and Fischer, 2000; Kim et al, 2004). Moreover, histological characterization of the brassinosteroid-related mutants, *de-etiolated2* (*det2*) and *dwarf1* (*dwf1*), showed that these two mutants are defective not only in leaf cell expansion but also in leaf cell proliferation preferentially along the leaf-length direction (Nakaya et al., 2002). Consistently, expression of *CYCD3;1* is induced by brassinosteroid in *det2* suspension culture (Hu et al., 2000). These observations suggest that there is at least some preference in the direction of cell division within the leaf blade.

In this study, I investigated a newly isolated dominant mutant, named *rot4-1D*, develops short and rounded leaves which are resulting from a decrease in cell proliferation along the leaf-length direction. *ROT4* encodes a plasma membrane-localized small polypeptide of 53 amino acid residues and defines a novel plant specific family of small peptides. This study will provide information for better understanding of the mechanism that links cell proliferation and leaf morphogenesis.

2 Materials and Methods

2.1 Plant Materials and Growth Conditions

The *rot4-1D* mutant was isolated in Landsberg *erecta* (*er*) background that also carried the weak *curly leaf* (*clf*) mutant allele, *clf-9* (Goodrich et al., 1997). The *rot4-1D* mutant was crossed to wild type Columbia three times to remove the *clf-9* and *er* alleles and an identical phenotype was observed, indicating that it was independent of the *clf* or *er* background. Because the *rot4-1D* inflorescence phenotype resembled that of *er*, absence of *er* mutation was confirmed by a sequence analysis of the *ER* locus. *clf* mutation was also removed from the *rot4-1D* mutant. For analyses of plants, seeds were sown on rock wool. After 24 h at 4°C in darkness, plants were grown under light at $40.4 \pm 6.7 \mu\text{mol/m}^2/\text{s}$ at 22°C. Ages of plants were given in terms of days after transfer to 22°C.

2.2 Anatomical Analysis

To observe palisade cells, leaf tissues were cleared with chloral hydrate solution (4 g/ml chloral hydrate and 0.4 g/ml glycerol) as described elsewhere (Tsuge et al., 1996). Individual cell sizes were measured using the ImageJ 1.29x program (National Institutes of Health; <http://rsb.info.nih.gov/ij/>).

2.3 Determination of the T-DNA Insertion Site in *rot4-1D*

To clone genomic DNA flanking the T-DNA insertion, plasmid rescue (Weigel et al., 2000) was performed. Genomic DNA was extracted from *rot4-1D* mutant plants, digested with *EcoRI* and ligated overnight under conditions favoring intramolecular ligation. The resulting plasmid, pJG28, contained both pSKI015 and plant genomic DNA sequences with a single *EcoRI* site. Sequence analysis of pJG28 using a primer designed from pSKI015 sequence indicated the approximate site of the T-DNA insertion. To confirm the precise T-DNA insertion site, the following oligonucleotides were used for polymerase-chain-reaction (PCR) amplification using *rot4-1D* genomic DNA as a template; ROT4RBsite, 5'-AAGCCGTTAGGTTTAGAGGG-3'; T7, 5'-GTAATACGACTCACTATAGGGC-3'. Amplified DNA

fragments were sequenced with the ROT4R site primer.

2.4 Determination of the Full-length *ROT4* cDNA Sequence

The full-length cDNA of *ROT4* was established by 5' rapid amplification of cDNA ends (RACE) and 3' RACE using 5' RACE System Version 2.0 (Invitrogen Corp., Carlsbad, CA, USA) and 3' RACE System (Invitrogen Corp.). Total RNAs were prepared from whole mature plants using the RNeasy Plant Mini Kit (QIAGEN Inc., Valencia, CA, USA). The following oligonucleotides were used as gene-specific primers 1 (GSP1) of PCR for 5' RACE; ROT4-R, 5'-TAATCAAGAGTCTTTGCGGTCG-3'; and as GSP2; 5RACE-GSP2, 5'-CGTGCCAGCAAACATAACATG-3'. For 3' RACE, the following oligonucleotides were used as GSP1 and GSP2; ROT4-F, 5'-ACAAATCAATGGCACCGGAG-3'; 3RACE-GSP2, 5'-TGAGCCGTGCAAGACTTTTG-3'.

2.5 Generation of Transgenic Lines Overexpressing *ROT4* Variants

Total RNAs were prepared from whole mature plants as above. The SuperScript One-step RT-PCR Kit (Invitrogen Corp.) was used for reverse-transcription PCR (RT-PCR) according to the manufacturer's protocol. The condition for amplification by RT-PCR was one cycle at 50°C for 15 min and 94°C for 2 min, then 35 cycles at 94°C for 15 s, 57°C for 30 s and 72°C for 60 s. ROT4-F and ROT4-R were used as primers for RT-PCR. The RT-PCR products were subcloned into pCR2.1 (Invitrogen Corp.), and the resultant vector was named ROT4/pCR2.1. To generate 35S::*ROT4-green fluorescence protein (GFP)* transgenic plants, the binary vector construct ROT4-GFP/pSMAB704 was first made as follows. *ROT4* DNA was PCR amplified from ROT4/pCR2.1 template DNA using the oligonucleotides; ROT4-Gly-F (5'-CAATGGCACCGGAGGAGAATG-3') and ROT4-Gly-R (5'-TTTCCATGGCACCTCCACCTCCACCTCCAGAGTCTTTGCGGTCGTGG-3') in order to remove the *ROT4* stop codon and to introduce an *NcoI* site and a glycine linker. The product was subcloned into pCR2.1 to produce ROT4-Gly/pCR2.1. ROT4-Gly/pCR2.1 was digested by *EcoRI*, blunted using a DNA Blunting Kit (TaKaRa Bio Inc., Otsu, Japan) and then digested with *NcoI*. The vector pTH2 (Niwa et al.,

1999) which carries the GFP gene under control of the cauliflower mosaic virus (CaMV) 35S promoter was digested with *SalI*, blunted as described above and then digested with *NcoI*. These two fragments were ligated to produce ROT-GFP/pTH2. pSMAB704 was digested with *HindIII* and *EcoRI* to remove the 35S:: β -glucuronidase gene and then ligated to the 35S::*ROT4-GFP* gene which was excised from ROT4-GFP/pTH by *HindIII* and *EcoRI* digestion. Similarly, plasmid vector constructs ROT4 Δ N/pCR2.1 and ROT4 Δ C/pCR2.1 were made as follows. *ROT4* Δ N DNA was PCR amplified from ROT4/pCR2.1 template DNA using the oligonucleotides; ROT4dN-F (5'-ATGACTTTTGGGCAAAGTGC-3') and ROT4-R in order to remove the N terminus region of ROT4 and to add the first methionine codon. *ROT4* Δ C DNA was PCR amplified using the oligonucleotides; ROT4-F and ROT4dC-R (5'-TCAGTCGTGCCAGCAAATA-3') in order to remove the C terminus region of ROT4 and to add the stop codon. Each DNA fragment was inserted in pCR2.1. The DNA fragment insertion to the binary vector pSMAB704 was performed as described for the case of *ROT4-GFP*. These constructs were introduced into wild-type plants by *Agrobacterium*-mediated transformation using the simplified floral dip method (Clough and Bent 1998). Transgenic plants were selected on Murashige and Skoog medium containing 2 mg/ml Gellan Gum (Wako, Osaka, Japan), 10 μ g/ml bialaphos (Shinyo-Sangyo, Tokyo, Japan) and 500 μ g/ml claforan (Aventis Pharma Ltd., Tokyo, Japan).

2.6 Semi-quantitative RT-PCR

Reverse transcriptions were carried out using the Super Script II RT and the adapter primer of the 3' RACE System. For amplification of *ROT4* cDNA, ROT4-F and ROT4-R were used. As a control, the following oligonucleotides were used to detect the constitutively expressed *ACTIN2* (*ACT2*) gene (An et al., 1996); ACT2-F, 5'-GAAATCACAGCACTTGCACC-3'; ACT2-R, 5'-AAGCCTTTGATCTTGAGAGC-3'. The condition for amplification by RT-PCR was one cycle at 50°C for 15min and 94°C for 2 min, then 27 cycles for *ROT4* cDNA amplification or 33 cycles for *ACT2* cDNA amplification, at 94°C for 15 s, 57°C for 30 s and 72°C for 60 s.

2.7 Observation of the Intracellular Localization of ROT4

The ROT-GFP/pTH2 construct was introduced into *Arabidopsis* plants by floral dip transformation, as above. The GFP fluorescence was observed under a confocal laser-scanning microscope, TCS SP2 (Leica, Wetzlar, Germany). To carry out a plasmolysis experiment, epidermal peel was immersed in 0.8 M mannitol solution for 2 h.

2.8 Microarray Analysis

Total RNAs were prepared from 25-days-old plant using RNeasy Plant Mini Kit. Gene chip ATH1 (Affymetrix, Santa Clara, CA, USA) was used as the probe array DNA for microarray analysis according to the manufacturers protocol.

2.9 Phylogenetic Analysis

DNA sequences, which are similar to *ROT4*, were obtained by TBLASTN searches at NCBI (<http://www.ncbi.nlm.nih.gov/BLAST/>). The deduced amino acid sequences of the conserved region of *ROT4* and the retrieved DNA sequences were aligned using the CLUSTAL W program (Thompson et al., 1994) and alignments were refined manually. For construction of a maximum-likelihood (ML) tree, a neighbor-joining (NJ) tree as the start tree was used for a local rearrangement search. Then, the NJdist and ProtML programs were used in MOLPHY, version 2.3b3, package (<http://www.ism.ac.jp/software/ismlib/softother.html>; Adachi and Hasegawa, 1996). The NJ tree was obtained with NJdist and the ML tree was obtained with ProtML. The local bootstrap probability of each branch was estimated using the ProtML program (Himi et al., 2001, Sakakibara et al. 2001).

2.10 Isolation of *rtfl4-1*, *osrtfl1-1* and *osrtfl2-1*

To find knockout mutants of *Arabidopsis* and rice for the coding region of *RTFL* members, BLASTN searches were performed at TAIR BLAST (<http://www.arabidopsis.org/Blast/>) or Mutant panel (<http://tos.nias.affrc.go.jp/~miyao/pub/tos17/>). In *Arabidopsis*, only one mutant that has an insertion of T-

DNA in the coding region of a *RTFL* family member was found in the SALK T-DNA insertion collection, namely accession SALK_089234 which carries an insertion in *RTFL4*. In *Oryza sativa* L., two mutants with a *Tos17* transposon insertion in the coding region of *RTFL4* were found from the Rice insertion mutant database (Miyao et al., 2003), and these *RTFL* members were named *OsRTFL1* and *OsRTFL2*, respectively. These candidate knockout mutant populations were kindly supplied by the Ohio *Arabidopsis* Stock Center (USA) and the Rice Genome Resource Center (NIAS, Japan). Each homozygous mutant was identified by PCR analysis of genomic DNA. To identify homozygotes for the T-DNA insertion in *RTFL4*, the following oligonucleotides were used; RTFL4-P, 5'-GTTCGTTACCCAATGGCTC-3'; RTFL4-N, 5'-TGTTTGTGCCAGCAAACGAG-3', LBb1, 5'-GCGTGGACCGCTTGCTGCAACT-3'. The primer pair of RTFL4-P and LBb1 specifically amplifies DNA from the insertion allele whereas the primer pair of RTFL4-P and RTFL4-N was used for identification of the non-insertional allele. Similarly, to identify homozygotes for *Tos-17* transposon insertions in the *OsRTFL1* and *OsRTFL2* genes, the following oligonucleotides were used; OSRTFL1-F, 5'-GCCTATGGTTTGGCATTG-3'; OSRTFL1-R, 5'-GCGCCTCGTCGTCGACGT-3'; OSRTFL2-F, 5'-ATGGCATATCCCCTCCTGT-3'; and OSRTFL2-R, 5'-TCGCTCCAGCGGAGCAACA-3'.

3 Results

3.1 Isolation and Phenotypic Characterization of the *rot4-1D* Mutant

An insertional mutagenesis was performed by transforming plants with the T-DNA containing plasmid pSKI015. Insertion of this T-DNA in intergenic regions frequently results in gain of function mutations that increase expression of flanking genes (Weigel et al, 2000). Seeds were harvested from 2000 individual primary transformants (T1 generation) and the resulting T2 families were screened for mutations affecting leaf morphology. One family segregated for a novel, short leaf phenotype in a ratio (61 mutants:18 wild-type) consistent with the presence of a single, dominant mutation. Because the mutagenesis was performed in a Landsberg *er* background that also carried the weak *clf* allele *clf-9* (Goodrich et al., 1997), the mutation was introduced into an *ER+* *CLF+* background by crossing three times to plants of Columbia ecotype. A similar dominant mutant phenotype was observed to segregate, indicating that the phenotype was independent of the *ER* or *CLF* genes. The mutation was designated *rot4-1D* and all subsequent morphological analysis involved comparison of *rot4-1D* and wild-type sibs in the introgressed Columbia background.

The leaf blade of *rot4-1D* was short and rounded (Fig. 1A). The reductions in leaf blade length and petiole length in *rot4-1D* were more severe than those in leaf blade width (Fig. 1B, Fig. 2A). In addition, the reduction in leaf blade length was more pronounced in leaves formed at later developmental stages (Fig. 1B, Fig. 2A). In addition to the effects on leaf blade and petiole, *rot4-1D* floral organs and inflorescence stems were also shorter than those of wild type (Fig. 1C, D, Fig. 2A). By contrast, there were no significant differences in morphological features between wild type and *rot4-1D* roots (data not shown).

To test whether the reduced leaf length in *rot4-1D* is due to a decrease in cell number or size or both, the numbers and sizes of the palisade cells in the first, third and fifth rosette leaves were measured. The leaf blades of *rot4-1D* had fewer cells than wild type did, and, as in the case of the leaf blade length, this was more evident in the leaves formed at later developmental stages (Fig. 2B). To relate the decrease in the cell number to the effect of *rot4-1D* on leaf shape (Fig. 2A), the palisade cell numbers in both the leaf-length

and -width directions were counted. Again, the number of palisade cells in the leaf-length direction in *rot4-ID* decreased in a similar fashion to the decrease in total cell number in the sub-epidermal layer (Fig. 2C). However, the cell numbers along the leaf-width direction in *rot4-ID* were not significantly different at any of the developmental stages examined (Fig. 2C). In addition, the palisade cell sizes in bottom, middle and top portions of first and third leaves in *rot4-ID* were comparable to the corresponding wild type leaves and portions (Fig. 1E, Fig. 2D). Although the cell size in the bottom portion of the fifth leaf in *rot4-ID* was smaller than that of wild type (Fig. 2D), this might be due to a retardation in fifth leaf expansion since *rot4-ID* plants grow slightly slower than wild type. Cells in older leaves of *rot4-ID* expanded to a similar extent to wild type cells.

Taken together, these results suggest that the main effect of the *rot4-ID* mutation is a decrease in cell proliferation along the leaf-length direction. The measurements of cell size and cell number do not account for the decrease in leaf-width (Fig. 2A). This discrepancy could be attributable to the combined effect of subtle decreases in the cell number in the leaf-width direction and cell size in *rot4-ID*. In fifth leaves, wild type and *rot4-ID* were indistinguishable with respect to the sizes and the shapes of palisade, sponge and epidermal cells when transverse sections were examined (data not shown).

3.2 Identification of *ROT4*

To test whether this insertion might cause the *rot4-ID* mutation, I analyzed the genetic linkage of a herbicide (bialaphos) resistance marker carried on the T-DNA with the mutant phenotype. All 68 mutants in the original T2 family were resistant, whereas the 18 wild-type plants were herbicide sensitive, consistent with the insertion being responsible for the *rot4-ID* mutation. To identify the affected gene, the DNA flanking the T-DNA insertion was isolated by plasmid rescue (see materials and methods). Sequence analysis indicated that the insertion was in an intergenic region on chromosome II between the genes At2g36980 and At2g36990 (Figure 3A). However, when the mRNA levels of these genes were determined by RT-PCR, expression levels were similar in *rot4-ID* and wild-type plants (data not shown), suggesting that neither gene was likely to be responsible for the *rot4-ID* phenotype. Because the interval between

these two genes was relatively long (about 4.5 kbp), I searched the region for potential open reading frames (ORFs). A TBLASTX search was performed using the genomic DNA sequence between the stop codon of At2g36980 and the stop codon of At2g36990 as a query and several cDNA sequences from *Arabidopsis* and other plant species were retrieved. Although none of them perfectly matched the query genomic sequence, on the basis of the alignments and conceptual translations, a small potential ORF that encodes 53 amino acid residues was identified (Figure 3A,B). The ORF was located within 1kb from the right border of the T-DNA insert. Because pSKI015 T-DNA insertions generally affect expression of genes adjacent to the T-DNA right-border which carries CaMV 35S enhancers (Weigel et al, 2000), it seemed likely that increased expression of this ORF was the basis of the dominant *rot4-1D* phenotype.

To test whether this small ORF was expressed in wild type, RT-PCR was carried out. As shown in Figure 3C, a cDNA band of the expected size was amplified. In addition, this mRNA accumulated at a higher level in *rot4-1D* than in wild type (Figure 3C). Because these results strongly suggest that ROT4 encodes this small ORF, its full-length sequence was determined by RACE PCR (GenBank accession number, AB107209). To confirm that this gene corresponded to *ROT4*, I tested whether the *rot4-1D* phenotype was reconstituted when wild-type plants were transformed with a construct that placed the candidate gene fused with GFP under control of the CaMV 35S promoter (*35S::ROT4-GFP*). Foliage leaves of homozygous T2 plants from three independent transformants were shorter than those of wild type as was seen in *rot4-1D* (Figure 3D), confirming that the candidate gene corresponded to *ROT4*.

3.3 Expression Pattern of *ROT4*

The *ROT4* expression pattern was examined in various organs of wild-type plants by RT-PCR analysis using *ROT4*-specific primer sets. Although *ROT4* was strongly expressed in flowers and flower buds, the accumulation of *ROT4* mRNA was not detected in mature rosette leaves (Figure 4A). In young seedlings, however, the expression of *ROT4* was clearly detected in shoots (Figure 4B). I next characterized the *ROT4* expression level in shoots of seedling at different developmental stages. After stratification, plants were incubated in dark condition for 2 days, and were then grown in light for several days. The *ROT4* expression

level in shoots of seedlings was highest at 6 days after the shift to light (Figure 4C). Using plants at this stage, the organ-specificity of *ROT4* expression was analyzed. The shoots of seedlings were dissected into the full-expanded cotyledons, the primordia of the first pair of foliage leaves, and shoot apices which included the shoot apical meristem and younger leaf primordia. The *ROT4* expression was highest in the shoot apices, and somewhat reduced in the leaf primordia (Figure 4D). Expression in the mature cotyledons was extremely low. These results confirmed that *ROT4* is expressed in wild-type leaves during early developmental stages.

3.4 Plasma Membrane Localization of ROT4

To determine the intracellular localization of the ROT4 protein, I examined young leaves of *35S::ROT4-GFP* transgenic *Arabidopsis* plants using confocal microscopy. As shown in Figure 5A and B, GFP signal was localized at the periphery of both palisade and epidermal cells in the transgenic *Arabidopsis* plants. The same localization was observed also in onion epidermal cells that were bombarded with the *35S::ROT4-GFP* transgene (Figure 5D). To determine whether the ROT4-GFP fusion was localized in the plasma membrane or in the cell walls, plasmolysis was induced with 0.8 M mannitol. ROT4-GFP localized with the shrunken plasma membrane, indicating that it was present in the plasma membrane and not in the cell wall (Figure 5C,D). Thus, unlike the *35S::GFP* control plants, in which the GFP fluorescence was mainly cytosolic (Figure 5E), the ROT4-GFP fusion protein was localized to the plasma membrane.

3.5 Microarray Analysis in *rot4-1D*

Over-expression of *ANT* extends the period of CycD3 expression in leaves and eventually leads to the formation of large leaves (Krizek, 1999; Mizukami and Fischer, 2000). Therefore, I expect that expression of some of the cell cycle-related genes might be altered in *rot4-1D*. To identify genes whose expression level was altered in *rot4-1D* mutants, a microarray analysis was carried out. Although cell proliferation activity is reduced in *rot4-1D*, expression levels of genes that control the cell proliferation such as cell cycle-related genes were not detectably altered. Several genes were dramatically up-regulated in *rot4-1D*

(Table 1) but the relationship between these genes and cell proliferation is unclear. There were no genes that were down-regulated below 10% levels of wild type gene expression (data not shown).

3.6 ROT4 Is a Member of a Novel, Seed Plant Specific Family of Small Peptides

Database searches revealed 22 other putative *Arabidopsis* proteins with similarity to ROT4. These proteins were named RTFL1 through 22 (ROT FOUR LIKE). Alignment revealed a 29 amino acid region that was conserved between the RTFL members (Figure 6A). The region was rich in basic amino acids and has not been previously identified in any other proteins of known function. I named the novel region RTF (ROT FOUR) domain. When a phylogenetic tree was produced from the RTF domain, no sub-classes were found between the RTFL members (Figure 6B). In other plant species such as *Oryza sativa*, *Glycine max*, *Populus balsamifera*, etc., there are ESTs that encode RTFL members (*O.s.*, AU182671; *G.m.*, AW458841; *P.b.*, BU880463). These hypothetical proteins were not found in non-seed plants and animals, suggesting that RTFL may be a seed plant-specific gene family.

Recently, Wen et al. (2004) reported that DVL family affect to *Arabidopsis* development especially the fruit shape. The DVL family corresponds to RTFL family; DVL1, DVL2, DVL3, DVL4 and DVL5 correspond to RTFL18, RTFL19, RTFL21, RTFL17 and RTFL15, respectively.

To further characterize RTFL function, in particular the loss of function phenotype, we screened existing collections of insertion mutants in *Arabidopsis* and rice for insertions that disrupted any RTFL member. Such mutations were very rare, presumably because the RTFL genes are extremely small, and I could not identify any insertion at ROT4. However a mutant that carried a T-DNA insertion within the ORF of *RTFL4* was identified within the SIGNAL collection of *Arabidopsis* T-DNA insertion lines (Figure 7A). The mutation is likely to be null because it disrupts the conserved RTFL domain and was designated *rtfl4-1*. Furthermore, I identified two mutants in *Oryza* (rice), that carried insertions of the *Tos17* transposon within *Oryza* homologues. These *Oryza* RTFL members were named *OsRTFL1* and *OsRTFL2*, and encoded proteins sharing 45 % and 38 % amino acid identity with ROT4 within the RTF domain, respectively (Figure 7B). The two rice mutants, also predicted to be severe loss of function alleles, were named *osrtfl1-1*

and *osrtf2-1*, respectively. I identified plants that were homozygotes for the various mutant alleles. However, none of the mutants showed any phenotype that I could discern, either in terms of organ shape or any other gross morphological character (Figure 7C, D). These results suggest that there might be functional redundancy between several or all RTFL members as might be expected given that the family comprises more than twenty members with similar protein sequences.

3.7 The RTF Domain Is Sufficient for ROT4 Activity

Although the RTF domain is conserved between distantly related plant species, the regions outside the RTF domain at the N-terminal and C-terminal ends of the protein are diverged. To investigate the function of the different domains of ROT4, I generated the constructs ROT4 Δ N or ROT4 Δ C which expressed modified proteins that lacked either the N-terminal or the C-terminal regions of ROT4, respectively (Figure 8A). The constructs were expressed under control of the CaMV 35S promoter in transgenic *Arabidopsis* plants. In both cases the resulting transgenic plants had short rosette leaves similar to those of *rot4-1D* mutants (Figure 8B). This result suggests that only the conserved RTF domain is required for ROT4 activity.

As in *rot4-1D* plants, which had short siliques, the transgenic plants also had short siliques. This phenotype was less severe for plants expressing ROT4 Δ N than for plants expressing ROT4 Δ C. Interestingly, the siliques of both of ROT4 Δ N and ROT4 Δ C over-expressing plants showed changed shape so that they resembled an arrowhead (Figure 8C). A similar phenotype was also reported for plants over-expressing the CYP78A9 gene, which encodes a cytochrome P450 enzyme or DVL family. In CYP78A9, the effects on silique shape were caused both by increased cell proliferation and also by increased cell enlargement in the carpel valves (Ito and Meyerowitz, 2000). Over-expression of DVL family leads the repression of expression level of MADS-box gene, *FRUITFULL* (*FUL*; Wen et al., 2004). It has known that the carpel cells in *ful* mutant decrease the cell size (Ferrández et al., 2000).

4 Discussion

4.1 ROT4 Is a Novel Small Peptide with a Conserved RTF Domain

I identified a novel gene that is over-expressed in an *Arabidopsis* mutant with short leaves (Figure 1). *ROT4* encodes a small peptide and its predicted molecular weight is only 6.2 kDa. Genome-wide database searches revealed that *ROT4* is a member of a novel gene family, which shares a 29 amino-acid domain, RTF. All these members encode small peptides. Small peptides are often involved in developmental or defense signaling. For example, CLAVATA3 (CLV3), phytosulfokine, S-locus cystein-rich protein/S-locus protein11, ENOD40, systemin, Brick1 (Brk1), rapid alkalization factor and POLARIS (PLS) have been described (Fletcher et al., 1999; Matsubayashi and Sakagami, 1996; Schopfer et al., 1999; Takayama et al., 2000; Yang et al., 1993; Pearce et al., 1991; Frank and Smith, 2002; Pearce et al., 2001; Casson et al., 2002). With the exception of Brk1 and PLS, these peptides are shown to act extracellularly as peptide hormones (Ryan et al., 2002). The action of Brk1 is unusual because it has no predictable targeting signals and functions non-cell autonomously. ROT4 represents another unusual example, since the ROT4-GFP fusion protein localized to the plasma membrane in onion epidermal cells (Figure 5). Given that ROT4 has neither a predictable signal peptide nor a transmembrane domain, it is likely that ROT4 is a peripheral membrane protein or a part of a plasma membrane-localized protein complex. Alternatively it may be transported across plasma membrane, since a cellular immune system, the transporter associated with antigen processing (TAP) transports peptides in the cytosol to the lumen of endoplasmic reticulum (Schmitt and Tampé, 2000). The RTF domain within the ROT4 peptide is likely sufficient for ROT4 activity, since transgenic plants expressing ROT4 Δ N or ROT4 Δ C truncations have short rounded leaves similar to those of the *rot4-ID* mutant (Figure 8B). This result indicates that other RTFL members may have similar activities, on account of their shared RTF domain, and suggests that there could be substantial functional redundancy between RTFL members.

4.2 Limitations of Conventional Genetic Screens for Identifying Small Genes

Because *ROT4* and *RTFL* genes have not been annotated in the *Arabidopsis* genome database, it is likely that many other novel small genes may be overlooked by gene prediction programs. In addition, the small size of their coding regions means that loss of function mutations are likely to be rare, so that the genes may not be disrupted in conventional mutagenesis programs. For example, I was able to identify only one insertion mutant amongst the 22 RTFL members in *Arabidopsis* despite the extensive collections that exist for reverse genetic analysis. Similarly, loss of function mutations affecting the *CLV3/ESR* (*embryo-surrounding region*)-related (*CLE*) gene family, which contains 28 members encoding small peptides (Cock and McCormick, 2001), are also extremely rare (Hobe et al, 2003). As well as the relative scarcity of mutations within small genes, redundancy between family members may also limit their identification in forward genetic screens. Consistent with this, it was striking that the *rtfl4-1*, *osrtfl1-1* and *osrtfl2-1* mutants were all without gross morphological phenotypes (Figure 7B). For identification of small genes and/or genes with functional redundancy, activation tagging has several advantages. Firstly, overexpression can often reveal a gain of function phenotype when loss of function mutations are without obvious phenotype (Wilson et al, 1996. Weigel et al, 2000). Secondly, because insertions that are very distant from the promoter (at least 3.6 kb upstream, Weigel et al, 2000) can give gain of function phenotypes, genes with small coding regions are nonetheless mutagenised as effectively as those with much larger coding regions. Thus activation tagging has recently proved an efficient means for identifying another class of small genes, those encoding microRNA (Palatnik et al, 2003).

4.3 The role of ROT4 in cell proliferation and leaf morphogenesis

When *ROT4* is over-expressed, cell numbers decreased specifically in the leaf-length direction (Figure 2, 3D). In addition other organs such as petals and sepals also showed a shortened, rounded shape, suggesting that *ROT4* over-expression may generally inhibit polar cell proliferation in lateral organs, specifically in the leaf-length direction (Figure 1C, D). As cell proliferation in the leaf-length direction in a leaf primordium continues as long as the leaf primordium grows (Donnelly et al., 1999). The mRNA of *ROT4* accumulated in wild-type shoot apices and leaf primordia, but was not detected in mature rosette leaves (Figure 4B, D).

Strong expression of *ROT4* was also detected in roots, flowers and flower buds, which like apices and young leaf primordial are regions of active cell proliferation. Because *ROT4* acts to restrict cell proliferation it is perhaps surprising that it is mainly expressed in regions of active cell proliferation. However, a precedent for this is provided by the *CINCINNATA (CIN)* gene of *Antirrhinum*, which is also involved in the control of leaf shape. The *CIN* gene is proposed to restrict cell proliferation by promoting cell cycle arrest, and it is also expressed in young leaf primordia in actively dividing regions of the leaf lamina (Nath et al., 2003). The expression of *CIN* moves in a wave that passes from tip to base of the leaf and that is correlated with a wave of cell cycle arrest and cell expansion that moves from tip to base. It will be interesting to observe the behaviour of the arrest front in *rot4-1D* mutants.

Two other factors that inhibit cell proliferation, *ICK1* and *KRP2*, have been analyzed in detail (Wang et al., 2000; De Veylder et al., 2001). These proteins bind to CDKA;1 and D-type cyclins, and inhibit the activity of cyclin-dependent kinase (Wang et al., 1998). The characteristic phenotypes of the respective over-expressers are that they show an extreme decrease in the number of cells per leaf blade (10% of wild type leaf cell number), and have serrated leaves. *ROT4* also exerts an inhibitory effect on cell proliferation. However, a critical difference compared with the over-expression of *ICK1* or *KRP2* is that the reduction in cell number caused by over-expression of *ROT4* is modest (Figure 2B; in the severest case, cell number of *rot4-1D* was 67.5% of that of wild type). Such differential inhibitory effects on cell proliferation may reflect different roles in the control of cell proliferation. Whereas *ICK1* and *KRP2* directly control key cell cycle components, it is likely that *ROT4* acts more indirectly. Firstly, *ROT4* is plasma membrane localized and therefore is likely to interact indirectly through a transduction pathway with the cell cycle machinery. In addition, *ROT4* and *RTFL* are a seed plant-specific gene family, suggesting they have evolved to control cell proliferation by a specialized manner.

Another important difference between plants over-expressing *ICK1* or *KRP2*, relative to *rot4-1D* is in the effect on individual cell sizes. In the previous reports, it was shown by the observations of transgenic plants expressing *ICK1*, *KRP2* or dominant negative CDKA;1 and also of *ant*, *swp*, *pfl2*, *G-protein a subunit 1 (gpa1)* and *gibberellic-acid insensitive (gai)* (Wang et al., 2000; De Veylder et al., 2001; Hermerly et al.,

1995; Mizukami and Fischer, 2000; Autran et al., 2002; Ito et al., 2000; Ullah et al., 2001; Tsukaya et al., 2002; reviewed in Tsukaya, 2003) that when the cell number of leaves decreases, compensatory increases in cell size occur, and the reduction of leaf size is consequently alleviated. This frequently observed phenomenon raised a possibility of the existence of a compensatory system between cell division and expansion. In *clf* leaves, both cell number and size decrease (Kim et al., 1998a). To best of our knowledge, *rot4-1D* is one of the very few instances of a mutant in which a decrease in cell number does not affect cell size. The only other example that I was aware of is the *ask1* mutant (Zhao et al., 1999). One simple interpretation of the *rot4-1D* phenotype is that a threshold value of reduction rate of cell number may exist to induce the compensation. It should be noted that some natural variations in leaf size and shape is solely attributable to changes in cell number (Tsukaya, 2002). Thus, it is also possible that ROT4 is involved in the control of organ shape and size. Further analysis of function of ROT4 and RTFL peptides should help us to understand how small peptides control development of plant organs. Another important question is whether individual leaf cells possess proliferation potential in leaf-length and leaf-width directions independently of one another. The *rot4-1D* phenotype is consistent with independent control of proliferation along the two axes. Observation of the cell division direction during leaf blade morphogenesis will provide more information to help answer this possibility.

Table 1 Genes up-regulated in *rot4-1D* identified by gene chip analysis^a

Encoded protein	Up-regulation (-fold: <i>rot4-1D</i> /wt) ^b	
	Experiment one	Experiment two
beta-glucosidase	29.86	27.86
expressed protein	34.30	21.11
glycine-rich protein	5.28	22.63
lipid transfer protein, putative	16.00	6.50
glycine-rich protein	11.31	5.28
caffeoyl-CoA 3-O-methyltransferase, putative	4.00	6.50
anther development protein	5.28	4.00
lipid transfer protein-like protein	5.66	2.64
xyloglucan endotransglycosylase, putative	4.29	2.83
glycine-rich protein	5.28	2.46
putative cysteine proteinase inhibitor B	4.29	3.25
putative hydrolase	3.48	3.73
oxidoreductase-like protein	3.03	4.00
hypothetical protein	3.73	2.14
family II extracellular lipase	3.03	2.64
ribosomal protein L16	2.14	3.48
ribosomal protein L14	2.00	3.03

^aGenes for which levels of transcripts were at least three times higher in *rot4-1D* than in wild type are shown.

^bRatio of transcript levels in the *rot4-1D* mutant to those in wild type.

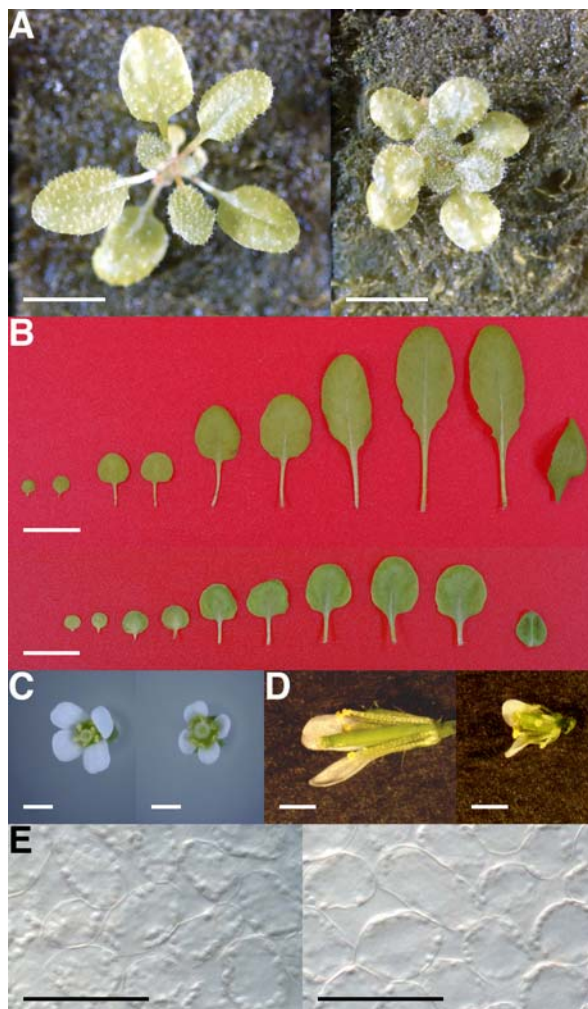


Figure 1 Phenotypes of *rot4-1D*.

(A) 25-days-old plants of wild type (left) and *rot4-1D* (right). Scale bars: 10 mm. (B) Leaves of 33-days-old plants of wild type (top) and *rot4-1D* (bottom). A cotyledon pair, first through seventh foliage leaves, and a cauline leaf are shown from left to right. Scale bars: 10 mm. (C) Top view of wild type (left) and *rot4-1D* (right) flowers. Scale bars: 1 mm. (D) Side view of wild type (left) and *rot4-1D* (right) flowers. Two sepals and petals were removed. Scale bars: 1 mm. (E) Palisade cells in middle portion of third foliage leaves of 38-day-old wild type (left) and *rot4-1D* (right). Scale bars: 0.1 mm.

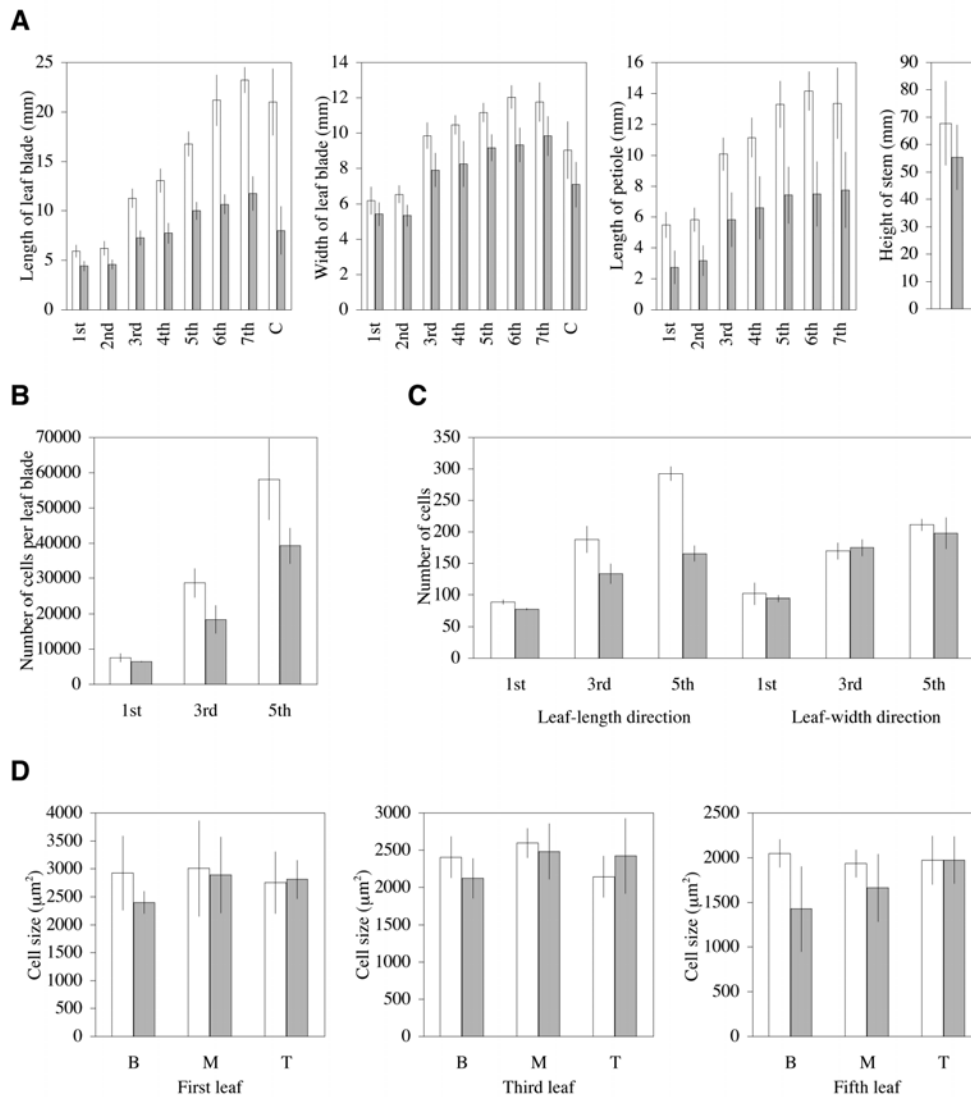


Figure 2 Measurements of leaf morphological characteristics in *rot4-1D*.

(A) Leaves and stems sizes were measured when individual plants had opened their third flower. Open column, wild type ($n = 14$); shaded column, *rot4-1D* ($n = 6$). Values are mean \pm SD. Numbers indicate the foliage leaf positions. C indicates cauline leaves. (B) Number of palisade cells in subepidermal layer per leaf blade. (C) Number of palisade cells in leaf-length direction and leaf-width directions. (B, C) Open column, wild type ($n = 3$); shaded column, *rot4-1D* ($n = 3$). Numbers indicate foliage leaf positions. Values are mean \pm SD. (D) Palisade cell size. Three independent experiments were carried out. In each case, cell area of 10 cells was measured. Three times using independent samples. Open column, wild type; shaded column, *rot4-1D*. Values are mean \pm SD. B, M and T indicate bottom, middle and top portions of a leaf, respectively.

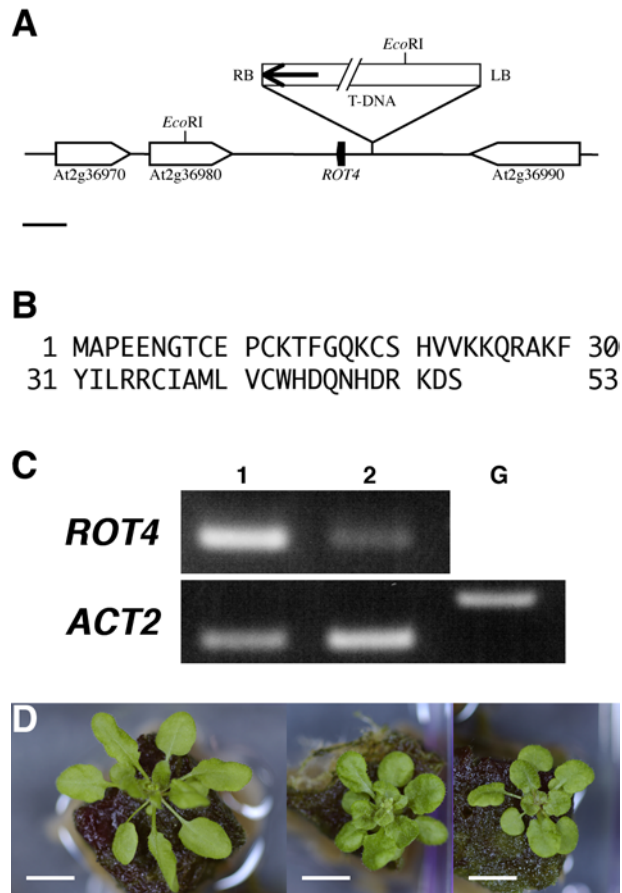


Figure 3 Structure of the *ROT4* locus and *ROT4* over-expression phenotype.

(A) A schematic map of the T-DNA insertion site in *rot4-ID*. An arrow indicates CaMV 35S enhancer. A bar indicates 1 kbp. (B) The deduced amino acid sequence of ROT4. (C) RT-PCR analysis of *ROT4* mRNA accumulation. Total RNAs of mature whole plants were used. Lane 1, *rot4-ID*; lane 2, wild type. The *ACT2* was used as a control. Lane G indicates a negative control using genomic DNA. (D) 30-day-old plants of wild type (left), *rot4-ID* (center) and transgenic T2 plants over-expressing *ROT4-GFP* (right). Scale bars: 10 mm.

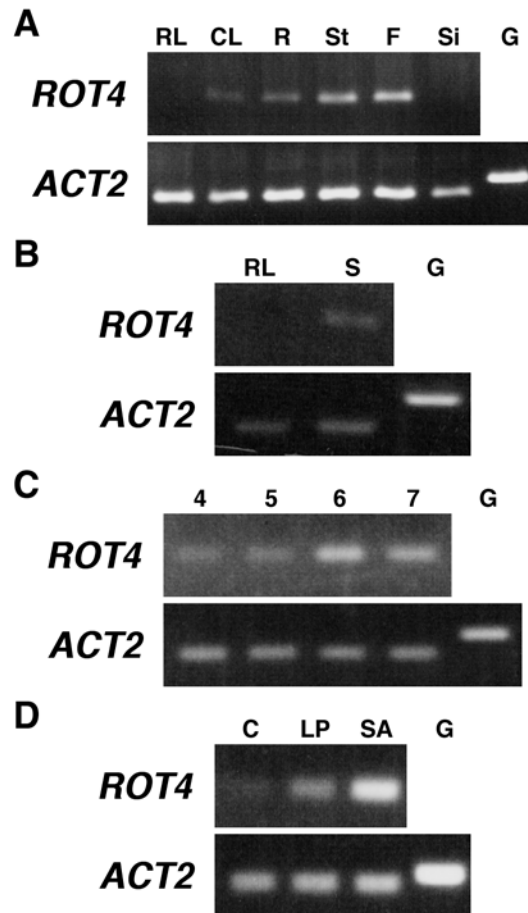


Figure 4 Expression of *ROT4*.

(A) Differential expression of *ROT4*. Total RNAs from following organs were analyzed. RL, rosette leaves; CL, cauline leaves; R, roots; St, stems; F, flowers and flower buds; Si, siliques. (B) *ROT4* mRNA accumulation in mature rosette leaves (RL) and shoots of 10-day-old seedlings (S). (C) *ROT4* mRNA accumulation in shoots of seedling at different stages. Etiolated seedlings grown 2 days in the dark were transferred to light condition and grown for several days. Numbers indicate days after shifting from the dark condition. (D) *ROT4* mRNA accumulation in shoots of seedling. C, cotyledons; LP, leaf primordia of first and second leaves; SA, shoot apices. G indicates negative controls using genomic DNA. The *ACT2* gene is expressed contitutively and is used a control for equivalent levels of cDNA amplification.

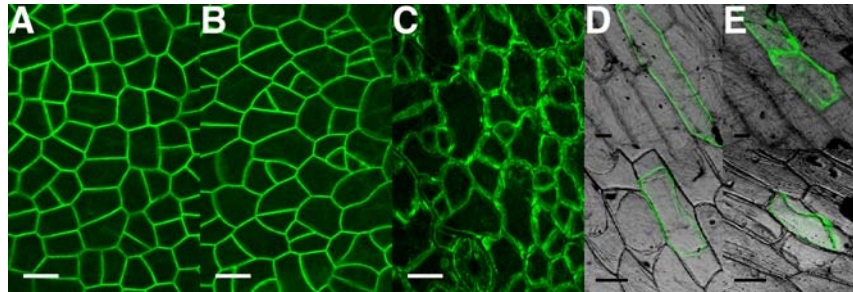


Figure 5 Intracellular localization of ROT4-GFP.

(A-C) Localization of ROT4-GFP fusion protein in mesophyll (A) and epidermal (B,C) cells of a young leaf primordium of a transgenic *Arabidopsis* plant harboring *35S::ROT4-GFP*. Cells were untreated (B) and treated with 0.8 M mannitol to cause osmosis (C). Scale bars = 10 μm . (D, E) Localization of ROT4-GFP fusion protein (D) and GFP protein (E) in onion epidermal cells. Fluorescent and Nomarski images are integrated for each panel. The upper panel shows cells untreated and the lower panel shows cells treated with 0.8 M mannitol. Scale bars = 100 μm . Note that the ROT4-GFP localized to the plasma membrane.

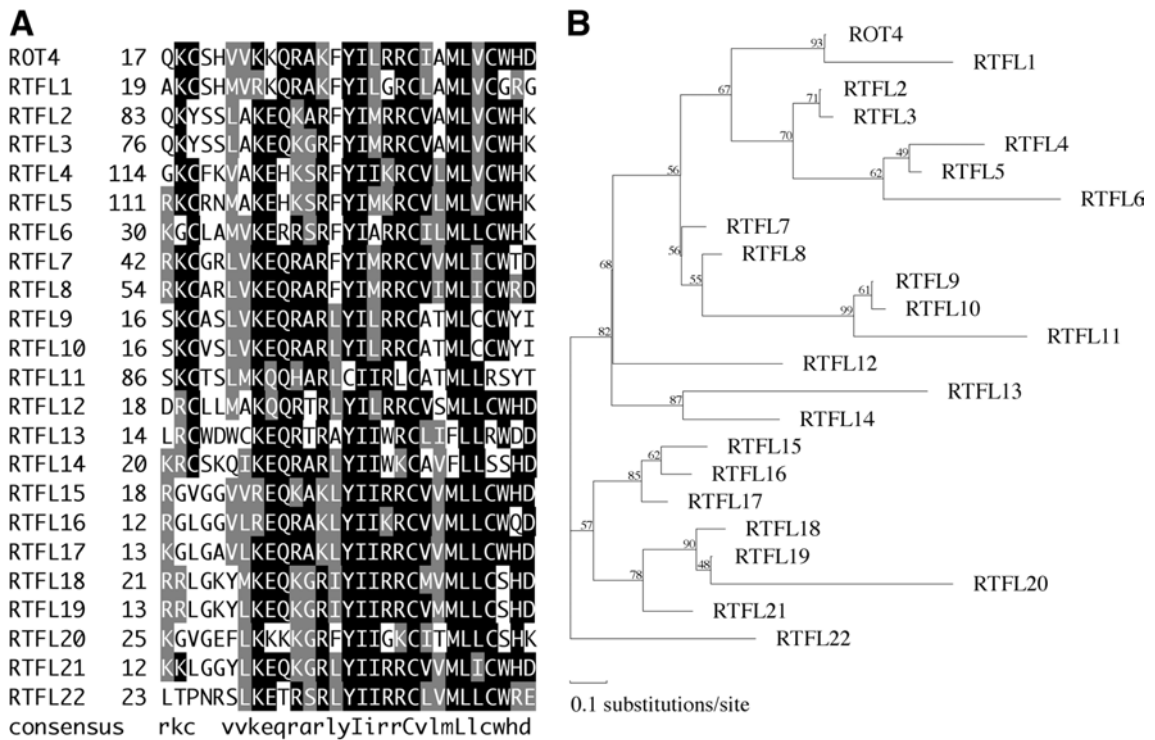


Figure 6 ROT4 gene family.

(A) The RTF domain of RTFL members in *Arabidopsis* genome. Numbers on the right of gene names indicate the positions of amino acid residues. Following Arabidopsis Genome Initiative (AGI) gene code have been assigned; RTFL2, At2g29125; RTFL3, At1g07490; RTFL5, At5g59510; RTFL8, At2g39705; RTFL16, At3g25717; RTFL17, At1g13245. Following members have an EST entry in GenBank; RTFL2, AV790691, AV825235; RTFL3, AU239065, AU239065; RTFL8, AU238463; RTFL10, AU237602; RTFL11, AU230682; RTFL12, AI997361, AV537172; RTFL15, AU227486, AU236535; RTFL16, T44697, T88458, Z17964; RTFL17, AI992996, AV534331, AV788885, AV832293, BU634921, T21221. (B) Phylogenetic tree of RTFL member. Numbers on branches indicate local bootstrap values, which were calculated with the ProtML program. The length of each horizontal branch is proportional to the estimated evolutionary distance.

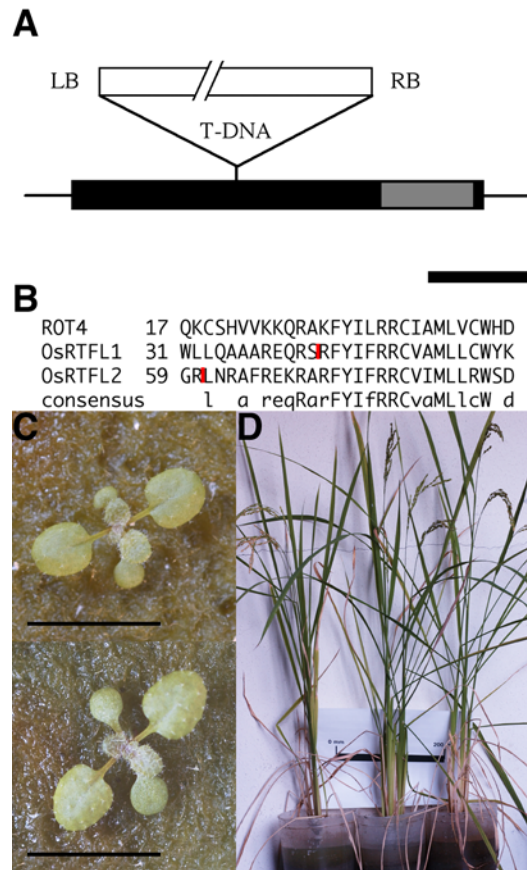


Figure 7 Knockout mutant of the members of ROT4 family.

(A) T-DNA insertion site within *RTFL4* in *Arabidopsis*. A solid rectangle and a shaded rectangle indicate a potential protein-coding region and a region encoding RTF domain of *RTFL4*, respectively. A bar indicates 100 bp. (B) The RTF domain of ROT4, OsRTFL1 and OsRTFL2. Numbers on the right of gene names indicate the positions of amino acid residues. Red lines indicate insertion sites of Tos17. (C) Top view of *rtfl-1* (top) and wild type (bottom) of *Arabidopsis*. Scale bars: 10 mm. (D) Side view of wild type (left), *osrtfl1-1* (center) and *osrtfl2-1* (right) of *Oryza*. Scale bar: 200 mm.

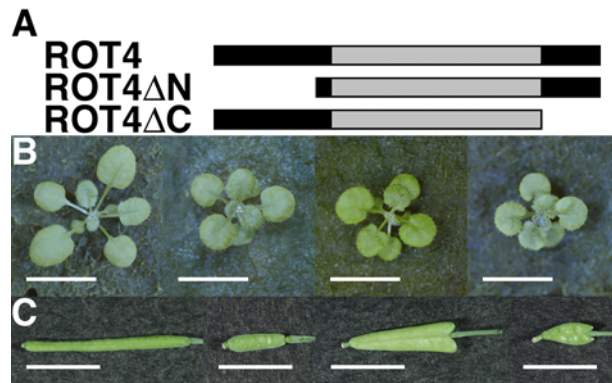


Figure 8 Phenotypes of transgenic plants over-expressing ROT4 Δ N and ROT4 Δ C.

(A) Primary structure of ROT4, ROT4 Δ N and ROT4 Δ C peptide. Solid rectangles and shaded rectangles indicate protein-coding regions and RTF domains of ROT4. (B) 25-day-old plants of wild type, *rot4-1D*, transgenic T2 plant over-expressing ROT4 Δ N and ROT4 Δ C are shown from left to right. Scale bars: 10 mm.

(C) The silique of wild type, *rot4-1D*, transgenic T2 plant over-expressing ROT4 Δ N and ROT4 Δ C are shown from left to right. Scale bars: 5 mm.

CHAPTER II

Development of Leaf Thickness Measurement Instrument and Anatomical Characterization of *Arabidopsis* Thick-leaf Mutant N692.

1 Introduction

Plant leaves have a polarity toward its thickness direction besides dorsoventral, longitudinal and mediolateral polarities. Diversity in leaf thickness reflects morphological adaptation of leaves to various environments. For example, succulent plants such as *Crassulaceae* and *Cactaceae* have thick leaves. Moreover, plants exhibit plasticity in leaf thickness. Leaves developed as sun leaves have more developed palisade tissue under high intensity of light, or as shade leaves that developed under low intensity of light have thinner palisade tissue than sun leaves (Esau, 1977). Yano and Terashima (2001) reported that light signals from mature leaves affect determination of anatomy of new leaves in *Chenopodium album*. In addition to light conditions, it is known that several phytohormones also affect the leaf thickness. Brassinolide, indoleacetic acid or gibberellin A3 treatment leads to a slight increase of height of leaf parenchyma and epidermal cells in *Tabebuia alba* (Ono et al., 2000). In *Arabidopsis thaliana*, the *de-etiolated-2 (det2)* mutant, which has a defect in steroid 5 α -reductase involved in brassinosteroid biosynthesis pathway (Li et al., 1996), has thick leaves compared with wild type (Ramonell et al., 2001), while Nakaya et al. (2002) did not recognize such a phenotype in *det2-13* and *det2-18* alleles. In tomato, leaves of *high pigment-1 (hp-1)* mutant are thicker than those of wild type, because *hp-1* mutation dramatically increases the periclinal elongation of palisade cells (Cookson et al., 2003). Despite these phenomena were confirmed in several plant species, the mechanisms for the leaf-thickness control are still unknown. Recently, it was reported that *HP-1* encodes a tomato homolog of the *Arabidopsis* UV-damaged DNA binding protein 1 (DDB1), and are shown to interact both biochemically and genetically with the nuclear localized protein, DET1 (Schroeder et al., 2002; Lieberman et al., 2004). However, the casual

relationship between HP-1 and the leaf-thickness was unclear, because phenotype of *hp-1* is pleiotropic.

Several examples in which cell proliferation or polarized expansion affect the leaf thickness have been known besides the effects of phytohormones. For example, the *angustifolia (an)* mutant, which has a defect in a gene for C-terminal Binding Protein homolog, develops leaf cells narrower and thicker than wild type (Tsuge et al., 1996). From the observation of mesophyll cells and the cortical microtubules in *an*, the orientation of the cortical microtubules altered (Kim et al., 2002). Because in plant cells, an orientation of cortical microtubules controls a direction of cell expansion (Cyr, 1994; Shibaoka, 1994), this result suggests that polar cell expansion controlled by microtubule organization may be important for the determination of the leaf thickness. Moreover, leaf thickness is known to be affected by some cell cycle regulatory genes. For example, when Kip-related protein 2 (KRP2) is over-expressed, leaf thickness is increased since so-called compensation (Tsukaya, 2002; Beemster, 2003) is triggered where the decrease of cell proliferation induces an increase of cell volume (De veylder et al., 2001). Although the decrease of cell number is occurred in the proximodistal and the mediolateral directions, the number of mesophyll-cell layers does not decrease and leaf cells expand a polar manner. The same phenomenon is also seen in tobacco overexpressing a dominant negative version of CDKA;1 (Hemerly et al., 1995).

The increase of leaf thickness observed in these examples, however, is thought as a secondary effect since these mutants and transgenic plants do not have thickness-specific phenotypes. Such mutants have not been reported yet. Therefore, studies concerning to the leaf thickness have fallen behind those for plane geometrical morphogenesis of leaves. This is in part because the measurement of leaf thickness requires complicated processing of samples. Therefore, to isolate mutants whose leaves are thicker or thinner than wild type, I developed a new equipment for rapid measurement of the leaf thickness using a laser displacement sensor.

This instrument was named Leaf Thickness Measurement Instrument (LTMI). Complicated steps in conventional method can be omitted by using LTMI. This enabled me to perform a high-throughput screening for mutants with altered leaf thickness. As a result, three mutants were isolated. N692 is a representative mutant and has a decreased cell number and an increased cell volume without alteration of

number of mesophyll layer. In this chapter, I describe the usefulness of LTMI and novel leaf-thickness mutants isolated by LTMI, which should serve as important materials for the better understandings of the thickness control.

2 Materials and Methods

2.1 Plant Materials and Growth Conditions

Arabidopsis wild type C24 (CS906) was obtained from the Arabidopsis Biological Resource Center (ABRC; Columbus, OH, U.S.A.). N692 mutant was crossed to C24 for back cross. For analyses of plants, seeds were sown on rock wool. Other environmental conditions are same as described in chapter I. For screening of mutant with altered leaf thickness, C24 T-DNA activation tagged pool (CS31401) was obtained from ABRC. The 3rd leaves of 30-day-old plants are measured by LTMI.

2.2 Equipments for LTMI

For construction of LTMI, a power supply (MS-H75), a programmable controller (KV-16DT), a laser displacement sensor (LK-2010), a graphic analog controller (RJ-800) and an A/D converter (NR-110) were prepared (all equipments were produced by Keyence Corp., Osaka, Japan). The power supply is a source of electric supply to the programmable controller, the laser displacement sensor and the graphic analog controller. CRY-2000 (Diversified Biotech, Boston, MA U.S.A) was used as a segment of white tape to ensure the correct reflection of the laser beam (Figure 9).

2.3 Anatomical Analyses

To observe palisade cells, leaf tissues were cleared with chloral hydrate solution as described in chapter I. For histological analysis, leaf or stem samples were fixed and embedded in Technovit 7100 (Kulzer, Hereaus). A series of 6 μ m thick transverse sections were made with a rotary microtome HM355S (Microm). Sections were stained with staining solution containing 0.5% toluidine blue and 0.1 % sodium carbonate and observed with microscope. Individual cell sizes were measured using the IMAGE J program described as chapter I.

3 Results

3.1 Development of Measurement Instrument of Leaf Thickness

Traditional measurement of *Arabidopsis* leaf thickness requires time consuming steps, such as fixation of leaves, dehydration, embedding of the samples, slicing by a microtome and observation under microscopes. Thus, I tried to develop an instrument, which can measure quickly the thickness of *Arabidopsis* living leaves.

As the first attempt, I used the coating thickness tester SDM-3000T (Sanko electronic laboratory Co. Ltd., Kawasaki, Japan), which measures a distance between a metal surface and the sensor probe. In theory, putting a piece of leaf on a metal plate and pressing the leaf surface with the sensor probe can measure a thickness of plant leaves. However, employment of the sensor probe of this tester was unsuitable for this purpose due to two problems. First, the diameter of sensor tip was too large (about ϕ 2 mm). This prevented the measurement from the correct positioning of a leaf sample. Second, measurement with the same pressing force, with which leaf piece is pushed onto a metal plate, at every experiments was difficult. Because *Arabidopsis* leaves are tender, pressing by the sensor probe crushed leaves. Moreover, when a degree of pressing force was altered manually, the different outputs were obtained depending on the intactness of leaf sample. Therefore, I tried another method. To solve the first problem, a laser displacement sensor LK-035 (Keyence Corp.; diameter of the laser, ϕ 30 μ m) was adopted. This sensor also solved the second problem since it is a non-destructive method. But the measurement of distance between the sensor and the surface of leaf tissue was difficult, probably because leaf epidermal cells and trichomes are transparent, and diffused reflection of the laser ray is occurred on the leaf surface. In order to obtain the appropriate laser reflection, the leaf sample was covered with a piece of white tape. The addition of this step gave successful reflection of the laser beam. This method was named Leaf Thickness Measurement Instrument (LTMI). Figure 9 shows the concept of LTMI.

To confirm the precision of LTMI, thickness of micro cover glass (Matsunami Ind. Ltd., Kishiwada, Japan; thickness, 0.12 ~ 0.17 mm) was tested, and the output values from LTMI are in the range of standard. This result indicates that LTMI can measure plate-like materials at high precision, and an artifactual effect by the

adoption of white tape is negligible if any.

Next, I tried the measurement of living leaf samples. Before measurement of thickness of a leaf, following preparations were needed. First, since the midrib is thicker than the other part of leaf lamina, it was removed by cutting with a razor blade, and then the leaf sample was mounted on a slide glass. Then a segment of white tape was overlaid on the surface of leaf sample, with a care not to remain air bubbles between them. Even using the LTMI, the presence of trichomes on the leaf surface severely affects the quality of the measurements, because LTMI is so sensitive to detect the air space made by the trichomes. Thus, all measurements were carried out for strains without trichomes, such as ecotype C24 or the *glabra1* (*gl1*) mutant of ecotype Columbia. To estimate the efficiency and accuracy of LTMI, I compared values of leaf thickness measured by the LTMI method and the conventional method. The output values obtained by these methods were slightly different. Since the conventional method requires dehydration, this may cause partial shrinkage of leaf samples (Table 2). Before screening of mutants associated with altered leaf thickness was carried out, another control experiment was done. When leaf thicknesses in *gl1an-1* double mutant and *gl1* single mutant were compared with LTMI method (Table 3), clear difference in the leaf thickness was found. Thus, LTMI is proven to be a suitable system for the rapid measurement of leaf thickness. Therefore, LTMI was used in following analyses.

3.2 Isolation and Anatomical Characterization of *Arabidopsis* Mutants with Altered Leaf Thickness

To isolate thick- or thin- leaf mutants of *Arabidopsis*, I carried out a genetic screening by using LTMI. Since mutant screening using activation tagging has several advantages, C24 T-DNA activation tagged pool was used. This mutant pool enables to isolate both loss- and gain-of-function mutants. In addition, genomic DNA sequences flanking T-DNA are easily determined by plasmid rescue. I expected that mutants with an increased leaf thickness due to an increased cell layer and/or an increased cell height will be isolated. Under the growth condition in this study, the number of leaf tissue layer is minimum. Therefore, thin-leaf mutants will be associated with the reduction of cell height. Thick-leaf mutants may have increased cell height and/or layer number. By screening 227 pools each containing 10 lines, I isolated three mutants from pool numbers

CS35692, CS35865 and CS36091. These mutants were named tentatively N692, N865 and N091, respectively (Figure 10). The leaf thicknesses of N692 or N865 were thicker and that of N091 was thinner than that of wild type. N692 was extreme mutant in terms of fold-change in thickness (Table 4; 1.25-, 1.11- and 0.90-fold leaf thickness in N692, N865 and N091, respectively). Thus, I choose N692 for further detailed analyses.

To find the cause of increased leaf thickness in N692, cross section of the mutant and wild type leaves was prepared and observed with microscope. Consistently, I found that the leaf thickness of N692 was 1.09-fold thicker than the wild type leaves (Figure 11 A,B; Table 4). The difference of the leaf thickness between wild type and N692 decreased compared with the measurement using by LTMI. This discrepancy may be caused by a difference of shrinkage of samples in the dehydration process during the preparation of the leaf section. Slicing of samples by microtome at right angle is difficult, and this may also be a cause of error. In N692, epidermal and mesophyll cells were larger than wild type. The height of cells in uppermost layer of the palisade tissue (subepidermal layer) was measured. The extent of the increase in the leaf thickness correlated with those of the cell height (Table 5), indicating that the increase of the leaf thickness in N692 is mainly caused by the cell expansion and is not by the increase of the mesophyll cell layer. Next, the area of the palisade cells from a paradermal viewpoint and the leaf blade area were measured (Figure 11 C,D; Table 6). Despite the cell area increased in N692, the leaf blade area did not differ between N692 and wild type, indicating that compensation occurred in N692. Stem thickness has also increased in N692 especially the expansion of epidermal cells is striking (Figure 12; Table 7).

4 Discussion

4.1 Usefulness of LTMI

In this study, LTMI was developed to measure the leaf thickness. This instrument allows the determination of leaf thickness easier and faster than the conventional method. Without this method, mutant screening based on leaf thickness should be impossible. As compared to the coating thickness tester which is necessary to touching to leaf samples, LTMI can measure soft leaf samples without crushing. However, there are some points to be improved. First, LTMI is not suitable to measure the thickness of a material with irregular surface; Arabidopsis leaves have a midrib, which is thicker than lamina portion, and numerous trichomes. Moreover, leaf epidermal cells cause diffused reflection of a laser beam. Therefore, measurement by LTMI requires removal of midrib and masking of leaf sample with opaque sheet. The optical problem may be able to solve by using supersonic waves displacement sensor (for example, E4PA-N; Omron Corp. Kyoto, Japan). Second, LTMI is applicable only to glabrous leaves. Since trichome prevents precise measurement, LTMI cannot be applied to standard wild type Columbia. This problem may not be solved without changing the fundamental approach.

4.2 Isolation of Arabidopsis Mutants with Altered Leaf Thickness

By using LTMI, I isolated three mutants N692, N865 and N091. However, I screened from only 227 pools each containing 10 lines. Although T-DNA is often inserted as multi copies (average 1.5 copy per line; Alonso et al., 2003) and activation tagging induces gene activation and disruption, the mutant screening performed in this study yielded genetic loci far from saturation. Thus, further screening should identify more genetic loci involved in the control of leaf thickness.

To understand a leaf thickness control in plants, mutants which increases or decreases cell proliferation and/or expansion along specifically leaf thickness direction are valuable. In order to isolate a mutant which decreases layer number, mutant screening under the condition to develop sun leaf may be needed.

N692 has expanded cells in epidermis and mesophyll layer along not only leaf thickness direction but also

leaf plane directions. In addition leaf cell number is reduced in N692. Therefore, phenotypes of N692 are different from what I had expected. However, mutants which mimic sun leaf or shade possibly exist in *Arabidopsis*.

4.3 Relationship between Leaf Thickness and Compensation

In N692, the cell volume increases while the cell number decreases. It is thought that compensation occurs. However, the decrease of the cell number occurs within each layer of leaf tissues. The increase of the cell volume is isotropic. As a result, the area of leaf blade is same as wild type while leaf thickness increases in N692. From these results, compensation does not occur such that leaf thickness is unchanged by the decrease in the number of tissue layer in N692.

Generally, compensation is triggered by the reduction in cell number (Tsukaya, 2003). However, fundamental defects in N692 should be carefully examined. For example, N692 has normal leaf area although most of known mutants with a decreased leaf cell number, such as *aintegumenta*, *struwwelpeter*, *pointed first leaf 2*, *gibberellic-acid insensitive* and *grf interacting factor1*, display incomplete compensation (Mizukami and Fischer, 2000; Autran et al., 2002; Ito et al., 2000; Tsukaya et al., 2002; Kim et al., 2004). As a rare example, Boudolf et al. (2004) recently reported that the transgenic lines expressing a dominant negative variant of B-type cyclin-dependent kinase repress the cell division in leaf, resulting the promotion of endoreduprecation and the increase of cell size, and the leaf blade area of the transgenic plants is as large as wild type. It is thought possibility that causes of N692 phenotype are in similar pathway to these transgenic plants. However, cell size and thickness in the stem are increased in N692 than in wild type. Therefore it remains possible that the enhanced cell expansion suppresses cell proliferation. To distinguish these possibilities, cloning of the N692 gene is necessary.

Table 2 Leaf thickness of mutants identified by LTMI.

	Output value as leaf thickness (μm)
LTMI method (n = 10)	134 \pm 8
Conventional method (n = 10)	125 \pm 19

Values represent the means \pm SD.

Table 3 Comparison of the leaf thickness in *gllan-1* and *gll* by using LTMI.

	<i>gllan-1</i> (n = 10)	<i>gll</i> (n = 10)
Leaf thickness (μm)	189 \pm 38	104 \pm 11

Values represent the means \pm SD.

Table 4 Leaf thickness of mutants identified by LTMI.

	Leaf thickness (μm)
LTMI method	
N692	
Mutant (n = 23)	158 \pm 10
Wild type (n = 27)	126 \pm 6
N865	
Mutant (n = 11)	130 \pm 5
Wild type (n = 12)	117 \pm 11
N091	
Mutant (n = 12)	105 \pm 9
Wild type (n = 12)	117 \pm 11
Cross section method	
N692	
Mutant (n = 10)	159 \pm 23
Wild type (n = 10)	146 \pm 18

Values represent the means \pm SD.

Table 5 Comparison of the leaf thickness and height of subepidermal layer in C24 and N692.

	N692	C24
Leaf thickness (μm)	159 \pm 23	146 \pm 18
Height of subepidermal layer (μm)*	35 \pm 6	32 \pm 5
Height of subepidermal layer / leaf thickness (%)	22	22

*Values represent the means \pm SEM for more than 8 plants.

Table 6 Comparison of the leaf blade area, palisade cell area and cell number.

	N692	C24
Leaf blade area (mm^2)	13.9 \pm 2.0	13.2 \pm 2.2
Cell area from a paradermal viewpoint (μm^2)*	2228 \pm 168	1502 \pm 281
Cell number per 1 mm^2	440 \pm 44	632 \pm 77

*Values represent the means \pm SEM for more than 8 plants.

Table 7 Comparison of the stem thickness in N692 and wild type.

	N692 (n = 7)	C24 (n = 7)
Stem thickness (mm^2)	1.16 \pm 0.15	0.93 \pm 0.15

Values represent the means \pm SD.

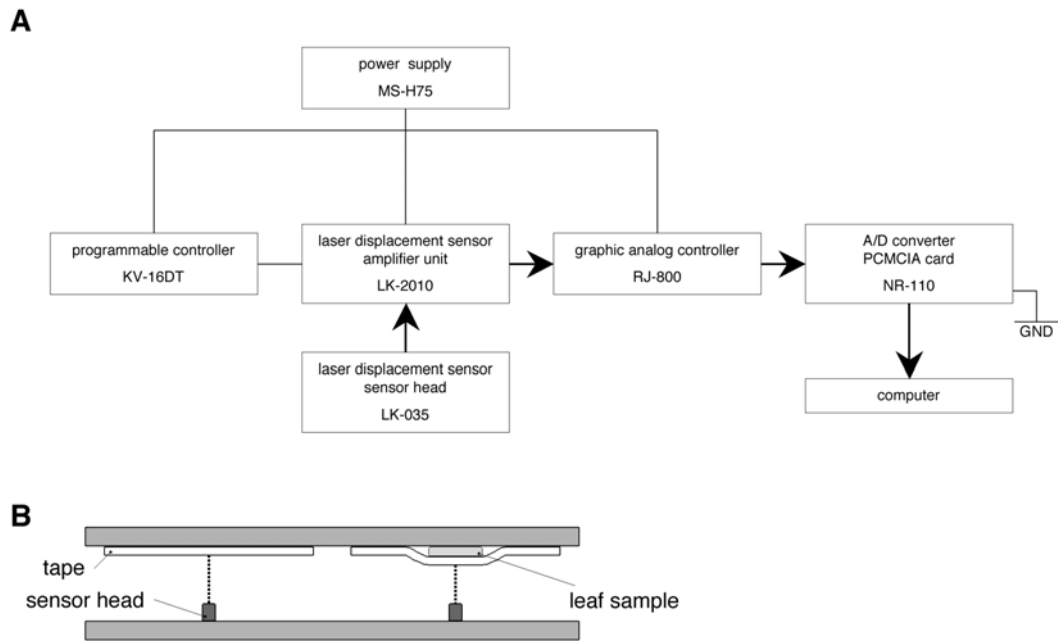


Figure 9 System Construction of LTMI.

(A) System construction diagram of LTMI. Power supply is a source of electronic supply to a programmable controller, a laser displacement sensor and a graphic analog controller. The programmable controller controls the laser displacement sensor. Arrows indicate a flow of signal of leaf thickness from a sensor head. GND indicates grounding (earthing). (B) A diagram showing the measurement with LTMI. A cover tape, a leaf sample and the sensor head are put between two stationary plates. The sensor head is fixed to the bottom plate. The cover tape adheres to top plate (left). To define zero point, distance from the sensor head to the surface of tape is measured. A leaf sample is held between the cover tape and the top plate (right). Actual leaf thickness is determined by subtracting the values measured with and without the leaf sample. Dotted lines indicate laser beam from the sensor head.

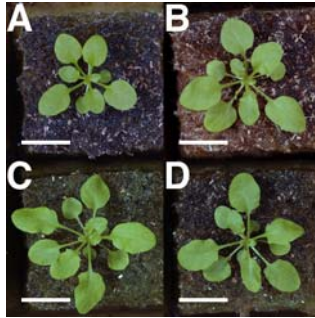


Figure 10 Mutants with altered leaf thickness.
(A) N692. (B) N865. (C) N091. (D) C24. Bars indicate 10 mm.

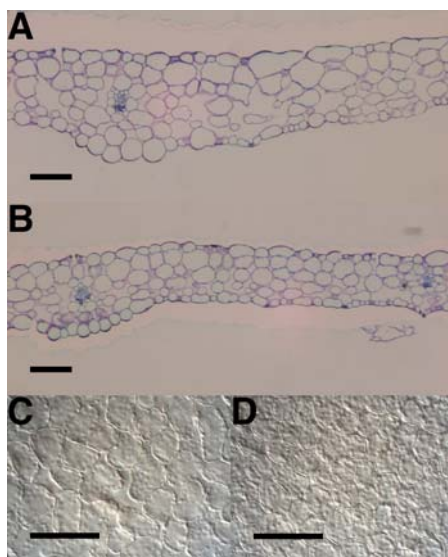


Figure 11 The Cell Shape in N692 Mesophyll Cells.

(A,B) Cross section of 1st leaf in N692 (A) and C24 (B). (C,D) Palisade cells from a paradermal viewpoint of 1st leaf in N692 (C) and C24 (D).

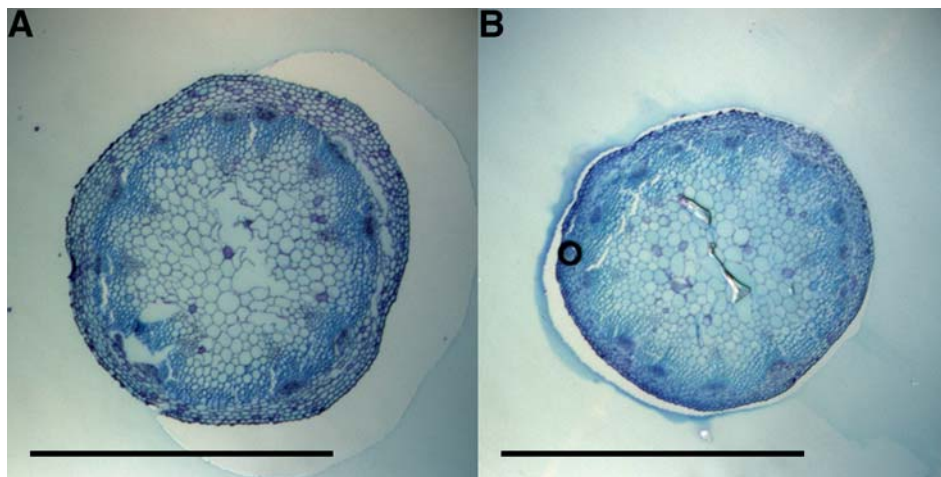


Figure 12 Cross section of N692 and wild-type stem.
(A) N692. (B) C24. Bars indicate 1 mm.

CONCLUSION

In this paper, the characterization of a short-leaf mutant *rot4-ID* and the isolation and analysis of a novel thick-leaf mutant N692 are reported in chapter I and chapter II, respectively.

From recent studies of the leaf morphogenesis with model plants, key factors involved in the size of leaf blade, the formation of serration, the establishment and maintenance of adaxial and abaxial identities, and the bilateral symmetry have been reported (Eshed et al., 2001; Klahre et al., 1998; Clarke et al., 1999; McConnell et al., 2001; Siegfried et al., 1999; Byrne et al., 2000). These studies collectively indicate that there are many regulatory pathways in the leaf morphogenesis. However, few studies have applied the concept of three-dimensional nature of leaves. For example, the existence of polarities along leaf-length and -width direction have been documented by the identification and developmental analyses of the *an* and *rot3* mutants (Tsuge et al., 1996). In addition, the finding of *ROT4* revealed that cell proliferation is also controlled by specific mechanisms along the leaf-length direction. A next interesting question about leaf-length control is whether *ROT3* and *ROT4* are controlled by the same mechanism that establishes the longitudinal polarity or these genes are independently regulated. This question will be answered by further functional analysis and isolation of novel mutants with short-leaf phenotype and with a defect in the establishment of longitudinal axis of the leaf. On the other hand, to best of my knowledge, this study is the first report for analysis of the leaf thickness control in *Arabidopsis*. Unfortunately, whether N692 and other mutants have a defect in a fundamental factors of leaf thickness control is remained unknown. However, since LTMI is an easy and accurate method, important genes for leaf thickness will be found out by further screening of mutants. Studies from many viewpoints are needed for understanding of the diversity of plant leaves. Moreover, studies from *Arabidopsis* have made it possible to describe a developmental phenomenon at organ, tissue, cell and molecular levels. As *Arabidopsis* began to be called reference plant, evo-devo studies that mutually analyze wild plants and model plants will further deepen our understanding of plant morphogenesis.

ACKNOWLEDGMENT

I thank Drs H. Tsukaya (NIBB, Okazaki, Japan) and G. Horiguchi (NIBB, Okazaki, Japan) for the experimental discussions. I also thank Drs J. Goodrich (ICMB, Edinburgh, UK), H. Ichikawa (NIAS, Tsukuba, Japan) and Y. Niwa (Shizuoka Prefectural University, Shizuoka, Japan) for the kind gifts of *rot4-ID* seed, pSMAB701 and pTH2, respectively. I also thank Dr T. Murata (NIBB, Okazaki, Japan) for his help to observe cells using a confocal laser-scanning microscope, Drs M. Hasebe (NIBB, Okazaki, Japan) and T. Nishiyama (NIBB, Okazaki, Japan) for their helps in the construction of a phylogenetic tree, Drs M. Kubo (RIKEN, Yokohama, Japan), T. Demura (RIKEN, Yokohama, Japan) and H. Fukuda (University of Tokyo, Tokyo, Japan) for their helps to operate in Gene tip analysis, Dr N. Ishikawa (NIBB, Okazaki, Japan) for isolations of *osrtfl1-1* and *osrtfl2-1*, and Ms E. Takabe (NIBB, Okazaki, Japan) for experimental assistances. The T-DNA insertion mutants at the *Arabidopsis RTFL4* locus and at the rice *OsRTFL1* and *OsRTFL2* loci were obtained from the collection of SALK T-DNA insertion lines (Ohio *Arabidopsis* Stock Center, USA) and Rice Genome Resource Center (NIAS, Japan), respectively.

REFERENCES

- Adachi, J. and Hasegawa, M.** (1996) MOLPHY version 2.3: programs for molecular phylogenetics based on maximum likelihood. *Comput. Sci. Monogr.* **28**, 1-150.
- Alonso, J.M., Stepanova, A.N., Leisse, T.J., Kim, C.J., Chen, H., Shinn, P., Stevenson, D.K., Zimmerman, J., Barajas, P., Cheuk, R., Gadrinab, C., Heller, C., Jeske, A., Koesema, E., Meyers, C.C., Parker, H., Prednis, L., Ansari, Y., Choy, N., Deen, H., Geralt, M., Hazari, N., Hom, E., Karnes, M., Mulholland, C., Ndubaku, R., Schmidt, I., Guzman, P., Aguilar-Henonin, L., Schmid, M., Weigel, D., Carter, D.E., Marchand, T., Risseuw, E., Brogden, D., Zeko, A., Crosby, W.L., Berry, C.C. and Ecker, J.R.** (2003). Genome-wide insertional mutagenesis of *Arabidopsis thaliana*. *Science* **301**, 653-657.
- An, Y.-Q., McDowell, J.M., Huang, S., McKinney, E.C., Chambliss, S. and Meagher, R.B.** (1996). Strong, constitutive expression of the Arabidopsis *ACT2/ACT8* actin subclass in vegetative tissues. *Plant J.* **10**, 107-121.
- Autran, D., Jonak, C., Belcram, K., Beemster, G.T., Kronenberger, J., Grandjean, O., Inzé, D. and Traas, J.** (2002). Cell numbers and leaf development in *Arabidopsis*: a functional analysis of the *STRUWWELPETER* gene. *EMBO J.* **21**, 6036-6049.
- Boudolf, V., Vlieghe, K., Beemster, G.T., Magyar, Z., Acosta, J.A., Maes, S., Van Der Schueren, E., Inzé, D. and De Veylder, L.** (2004). The plant-specific cyclin-dependent kinase CDKB1;1 and transcription factor E2Fa-DPa control the balance of mitotically dividing and endoreduplicating cells in *Arabidopsis*. *Plant Cell* **16**, 2683-2692.
- Beemster, G.T., Fiorani, F. and Inzé, D.** (2003). Cell Cycle: the key to plant growth control? *Trends Plant Sci.* **8**, 154-158.
- Byrne, M.E., Barley, R., Curtis, M., Arroyo, J.M., Dunham, M., Hudson, A. and Martienssen, R.A.** (2000). *Asymmetric leaves1* mediates leaf patterning and stem cell function in *Arabidopsis*. *Nature* **408**, 967-971.
- Byrne, M.E., Simorowski, J. and Martienssen, R.A.** (2002). *ASYMMETRIC LEAVES1* reveals *knox* gene redundancy in *Arabidopsis*. *Development* **129**, 1957-1965.
- Casson, S.A., Chilly, P.M., Topping, J.F., Evans, I.M., Souter, M.A. and Lindsey, K.** (2002). The *POLARIS* gene of *Arabidopsis* encodes a predicted peptide required for correct root growth and leaf vascular patterning. *Plant Cell* **14**, 1705-1721.
- Cho, H.-T. and Cosgrove, D.J.** (2000). Altered expression of expansin modulates leaf growth and pedicel abscission in *Arabidopsis thaliana*. *Proc. Natl. Acad. Sci. USA* **97**, 9783-9788.
- Clarke, J.H., Tack, D., Findlay, K., Van Montagu, M. and Van Lijsebettens, M.** (1999). The *SERRATE* locus controls the formation of the early juvenile leaves and phase length in *Arabidopsis*. *Plant J.* **20**, 493-501.
- Clough, S.J. and Bent, A.F.** (1998). Floral dip: a simplified method for *Agrobacterium*-mediated transformation of *Arabidopsis thaliana*. *Plant J.* **16**, 735-743.
- Cock, M.J. and McCormick, S.** (2001). A large family of genes that share homology with *CLAVATA3*. *Plant Physiol.* **126**, 939-942.
- Cookson, P.J., Kiano, J.W., Shipton, C.A., Fraser, P.D., Romer, S., Schuch, W., Bramley, P.M. and Pyke, K.A.** (2003) Increases in cell elongation, plastid compartment size and phytoene synthase activity underlie the phenotype of the *high pigment-1* mutant of tomato. *Planta* **217**, 896-903.

- Cyr, R.J.** (1994). Microtubules in plant morphogenesis: role of the cortical array. *Annu. Rev. Cell. Biol.* **10**, 153-180.
- De Veylder, L., Beeckman, T., Beeemster, G.T., Krols, L., Terras, F., Landrieu, I., Van Der Schueren, E., Maes, S., Naudts, M. and Inzé, D.** (2001). Functional analysis of cyclin-dependent kinase inhibitors of *Arabidopsis*. *Plant Cell* **13**, 1653-1668.
- De Veylder, L., Beeckman, T., Beeemster, G.T., de Almeida Engler, J., Ormenese, S., Maes, S., Naudts, M., Van Der Schueren, E., Jacqumard, A., Engler, G. and Inzé, D.** (2002). Control of proliferation, endoreduplication and differentiation by the *Arabidopsis* E2Fa-DPa transcription factor. *EMBO J.* **21**, 1360-1368.
- Dennison, K.L., Robertson, W.R., Lewis, B.D., Hirsch, R.E., Sussman, M.R. and Spalding, E.P.** (2001). Functions of AKT1 and AKT2 potassium channels determined by studies of single and double mutants of *Arabidopsis*. *Plant Physiol.* **127**, 1012-1019.
- Dewitte, W., Riou-Khamlichi, C., Scofield, S., Healy, J.M., Jacqumard, A., Kilby, N.J. and Murray J.A.** (2003). Altered cell cycle distribution, hyperplasia, and inhibited differentiation in *Arabidopsis* caused by the D-type cyclin CYCD3. *Plant Cell* **15**, 79-92.
- Donnelly, P.M., Bonetta, D., Tsukaya, H., Dengler, R.E. and Dengler, N.G.** (1999). Cell cycling and cell enlargement in developing leaves of *Arabidopsis*. *Dev. Biol.* **215**, 407-419.
- Elumalai, R.P., Nagpal, P. and Reed, J.W.** (2002). A mutation in the *Arabidopsis* *KT2/KUP2* potassium transporter gene affects shoot cell expansion. *Plant Cell* **14**, 119-131.
- Esau, K.** (1977) *Plant Anatomy of Seed Plants*. 2nd Edition. p. 351. John Wiley & Sons, Inc. New York.
- Eshed, Y., Baum, S.F., Perea, J.V., and Bowman, J.L.** (2001). Establishment of polarity in lateral organs of plants. *Curr Biol.* **11**, 1251-1260.
- Ferrándiz, C., Liljegren, S.J. and Yanofsky, M.F.** (2000). Negative regulation of the *SHATTERPROOF* genes by *FRUITFULL* during *Arabidopsis* fruit development. *Science* **289**, 436-438.
- Fletcher, J.C., Brand, U., Running, M.P., Simon, R. and Meyerowitz, E.M.** (1999). Signaling of cell fate decisions by *CLAVATA3* in *Arabidopsis* shoot meristems. *Science* **283**, 1911-1914.
- Folkers, U., Kirik, V., Schobinger, U., Falk, S., Krishnakumar, S., Pollock, M.A., Oppenheimer, D.G., Day, I., Reddy, A.S., Jurgens, G. and Hulskamp, M.** (2002). The cell morphogenesis gene *ANGUSTIFOLIA* encodes a CtBP/BARS-like protein and is involved in the control of the microtubule cytoskeleton. *EMBO J.* **21**, 1280-1288.
- Frank, M.J. and Smith, L.G.** (2002). A small, novel protein highly conserved in plants and animals promotes the polarized growth and division of maize leaf epidermal cells. *Curr. Biol.* **12**, 849-853.
- Goodrich, J., Puangsomlee, P., Martin, M., Long, D., Meyerowitz, E.M. and Coupland, G.** (1997). A polycomb-group gene regulates homeotic gene expression in *Arabidopsis*. *Nature* **386**, 44-51.
- Hemerly, A., Engler, J. de A., Bergounioux, C., Van Montagu, M., Engler, G., Inzé, D. and Ferreira, P.** (1995). Dominant negative mutants of the Cdc2 kinase uncouple cell division from iterative plant development. *EMBO J.* **14**, 3925-3936.
- Himi, S., Sano, R., Nishiyama, T., Tanahashi, T., Kato, M., Ueda, K. and Hasebe, M.** (2001). Evolution of MADS-box gene induction by *FLO/LFY* genes. *J. Mol. Evol.* **53**, 387-393.

- Hobe, M., Muller, R., Grunewald, M., Brand, U. and Simon, R.** (2003). Loss of CLE40, a protein functionally equivalent to the stem cell restricting signal CLV3, enhances root waving in *Arabidopsis*. *Dev. Genes Evol.* **213**, 371-381.
- Hu, Y., Bao, F. and Li, J.** (2000). Promotive effect of brassinosteroids on cell division involves a distinct *CycD3*-induction pathway in *Arabidopsis*. *Plant J.* **24**, 693-701.
- Ito, T., Kim, G.-T. and Shinozaki, K.** (2000). Disruption of an *Arabidopsis* cytoplasmic ribosomal protein S13-homologous gene by transposon-mediated mutagenesis causes aberrant growth and development. *Plant J.* **22**, 257-264.
- Ito, T. and Meyerowitz, E.M.** (2000). Overexpression of a gene encoding a cytochrome P450, CYP78A9, induces large and seedless fruit in *Arabidopsis*. *Plant Cell* **12**, 1541-1550.
- Iwakawa, H., Ueno, Y., Semiarti, E., Onouchi, H., Kojima, S., Tsukkaya, H., Hasebe, M., Soma, T., Ikezaki, M., Machida, C. and Machida, Y.** (2002). The *ASYMMETRIC LEAVES2* gene of *Arabidopsis thaliana*, required for formation of a symmetric flat leaf lamina, encodes a member of a novel family of proteins characterized by cysteine repeats and a leucine zipper. *Plant Cell Physiol.* **43**, 467-478.
- Kerstetter, R.A., Bollman, K., Taylor, R.A., Bomblies, K. and Poethig, R.S.** (2001). *KANADI* regulates organ polarity in *Arabidopsis*. *Nature* **411**, 706-709.
- Kim, G.-T., Fujioka, S., Kozuka, T., Tax, F.E., Takatsuto, S., Yoshida, S. and Tsukaya, H.** CYP90C1 and CYP90D1 are involved in different steps in the brassinosteroid biosynthesis pathway in *Arabidopsis thaliana*. *Plant J.* in press.
- Kim, G.-T., Shoda, K., Tsuge, T., Cho, K.-H., Uchimiya, H., Yokoyama, R., Nihitani, K. and Tsukaya, H.** (2002). The *ANGUSTIFOLIA* gene of *Arabidopsis*, a plant *CtBP* gene, regulates leaf-cell expansion, the arrangement of cortical microtubules in leaf cells and expression of a gene involved in cell-wall formation. *EMBO J.* **21**, 1267-1279.
- Kim, G.-T., Tsukaya, H., Saito, Y. and Uchimiya, H.** (1999). Changes in the shapes of leaves and flowers upon overexpression of cytochrome P450 in *Arabidopsis*. *Proc. Natl. Acad. Sci. USA* **96**, 9433-9437.
- Kim, G.-T., Tsukaya, H. and Uchimiya, H.** (1998a). The *CURLY LEAF* gene controls both division and elongation of cells during the expansion of the leaf blade in *Arabidopsis thaliana*. *Planta* **206**, 175-183.
- Kim, G.-T., Tsukaya, H. and Uchimiya, H.** (1998b). The *ROTUNDIFOLIA3* gene of *Arabidopsis thaliana* encodes a new member of the cytochrome P-450 family that is required for the regulated polar elongation of leaf cells. *Genes Dev.* **12**, 2381-2391.
- Kim, J.H. and Kende, H.** (2004). A transcriptional coactivator, AtGIF1, is involved in regulating leaf growth and morphology in *Arabidopsis*. *Proc. Natl. Acad. Sci. USA* **101**, 13374-13379.
- Klahre, U., Noguchi, T., Fujioka, S., Takatsuto, S., Yokota, T., Nomura, T., Yoshida, S. and Chua, N.H.** (1998). The *Arabidopsis* *DIMINUTO/DWARF1* gene encodes a protein involved in steroid synthesis. *Plant Cell* **10**, 1677-1690.
- Krizek B.A.** (1999). Ectopic expression of *AINTEGUMENTA* in *Arabidopsis* plants results in increased growth of floral organs. *Dev Genet.* **25**, 224-236.
- Li, J., Nagpal, P., Vitart, V., McMorris, T.C. and Chory, J.** (1996) A role for brassinosteroids in light-dependent development of *Arabidopsis*. *Science* **272**, 398-401.
- Lieberman, M., Segev, O., Gilboa, N., Lalazar, A. and Levin, I.** (2004) The tomato homolog of the gene encoding UV-damaged DNA binding protein 1 (DDB1) underlined as the gene that causes the *high pigment-1*

mutant phenotype. *Theor. Appl. Genet.* **108**, 1574-1581.

Matsubayashi, Y. and Sakagami, Y. (1996). Phytosulfokine, sulfated peptides that induce the proliferation of single mesophyll cells of *Asparagus officinalis* L. *Proc. Natl. Acad. Sci. USA* **93**, 7623-7627.

McConnell, J.R., Emery, J., Eshed, Y., Bao, N., Bowman, J. and Barton, M.K. (2001). Role of *PHABULOSA* and *PHAVOLUTA* in determining radial patterning in shoots. *Nature* **411**, 709-713.

Miyao, A., Tanaka, K., Murata, K., Sawaki, H., Takeda, S., Abe, K., Shinozuka, Y., Onosato, K. and Hirochika, H. (2003). Target site specificity of the Tos17 retrotransposon shows a preference for insertion within genes and against insertion in retrotransposon-rich regions of the genome. *Plant Cell* **15**, 1771-1780.

Mizukami, Y. and Fischer, R.L. (2000). Plant organ size control: *AINTEGUMENTA* regulates growth and cell numbers during organogenesis. *Proc. Natl. Acad. Sci. USA* **97**, 942-947.

Nakaya, M., Tsukaya, H., Murakami, N. and Kato, M. (2002). Brassinosteroids control the proliferation of leaf cells of *Arabidopsis thaliana*. *Plant Cell Physiol.* **43**, 239-244.

Nath, U., Crawford, B.C., Carpenter, R. and Coen, E. (2003). Genetic control of surface curvature. *Science* **299**, 1404-1407.

Nicol, F., His, I., Jauneau, A., Vernhettes, S., Canut, H. and Höfte, H. (1998). A plasma membrane-bound putative endo-1,4- β -D-glucanase is required for normal wall assembly and cell elongation in *Arabidopsis*. *EMBO J.* **17**, 5563-5576.

Niwa, Y., Hirano, T., Yoshimoto, K., Shimizu, M. and Kobayashi, H. (1999). Non-invasive quantitative detection and applications of non-toxic, S65T-type green fluorescent protein in living plants. *Plant J.* **18**, 455-463.

Ono, E.O., Nakamura, T., Machado, S.R. and Rodrigues, J.D. (2000) Application of brassinosteroid to *Tabebuia alba* (Bignoniaceae) plants. *Revista Brasileira de Fisiologia Vegetal* **12**, 187-194.

Palatnik, J.F., Allen, E., Wu, X., Schommer, C., Schwab, R., Carrington, J.C., and Weigel, D. (2003). Control of leaf morphogenesis by microRNAs. *Nature* **425**, 257-263.

Pearce, G., Strydom, D., Johnson, S. and Ryan, C.A. (1991). A polypeptide from tomato leaves induces wound-inducible proteinase inhibitor proteins. *Science* **253**, 895-898.

Pearce, G., Moura, D.S., Stratmann, J. and Ryan, C.A. Jr. (2001). RALF, a 5-kDa ubiquitous polypeptide in plants, arrests root growth and development. *Proc. Natl. Acad. Sci. USA* **98**, 12843-12847.

Ramonell, K.M., Kuang, A., Porterfield, D.M., Crispi, M.L., Xiao, Y., McClure, G. and Musgrave, M.E. (2001) Influence of atmospheric oxygen on leaf structure and starch deposition in *Arabidopsis thaliana*. *Plant Cell Environ.* **24**, 419-428.

Ryan, C.A., Pearce, G., Scheer, J. and Moura, D.S. (2002). Polypeptide hormones. *Plant Cell* **14**, (suppl.) S251-S264.

Sakakibara, K., Nishiyama, T., Kato, M. and Hasebe, M. (2001). Isolation of homeodomain-leucine zipper genes from the moss *Physcomitrella patens* and the evolution of homeodomain-leucine zipper genes in land plants. *Mol. Biol. Evol.* **18**, 491-502.

Sawa, S., Watanabe, K., Goto, K., Liu, Y.G., Shibata, D., Kanaya, E., Morita, E.H. and Okada, K. (1999). *FILAMENTOUS FLOWER*, a meristem and organ identity gene of *Arabidopsis*, encodes a protein with a zinc finger and HMG-related domains. *Genes Dev.* **13**, 1079-1088.

- Schmitt, L. and Tampé, R.** (2000). Affinity, specificity, diversity: a challenge for the ABC transporter TAP in cellular immunity. *Chembiochem*. **1**, 16-35.
- Schopfer, C.R., Nasrallah, M.E. and Nasrallah, J.B.** (1999). The male determinant of self-incompatibility in *Brassica*. *Science* **286**, 1697-1700.
- Schroeder, D.F., Gahrtz, M., Maxwell, B.B., Cook, R.K., Kan, J.M., Alonso, J.M., Ecker, J.R. and Chory, J.** (2002) Deetiolated1 and damaged DNA binding protein 1 interact to regulate *Arabidopsis* photomorphogenesis. *Curr. Biol.* **12**, 1462-1472.
- Semiarti, E., Ueno, Y., Tsukaya, H., Iwakawa, H., Machida, C. and Machida, Y.** (2001). The *ASYMMETRIC LEAVES2* gene of *Arabidopsis thaliana* regulates formation of a symmetric lamina, establishment of venation and repression meristem-related homeobox genes in leaves. *Development* **128**, 1771-1783.
- Shibaoka, H.** (1994). Plant hormone-induced changes in the orientation of cortical microtubules: alterations in the cross-linking between microtubules and the plasma membrane. *Annu. Rev. Plant Physiol. Plant Mol. Biol.* **45**, 527-544.
- Siegfried, K.R., Eshed, Y., Baum, S.F. Otsuga, D., Drews, G.N. and Bowman, J.L.** (1999). Members of the *YABBY* gene family specify abaxial cell fate in *Arabidopsis*. *Development* **126**, 4117-4128.
- Sugimoto-Shirasu, K., Stacey, N.J., Corsar, J., Roberts, K. and McCann M.C.** (2002). DNA topoisomerase VI is essential for endoreduplication in *Arabidopsis*. *Curr. Biol.* **12**, 1782-1786.
- Sugimoto-Shirasu, K. and Roberts, K.** (2003). "Big it up": endoreduplication and cell-size control in plants. *Curr. Opin. Plant Biol.* **6**, 544-553.
- Sun, Y., Zhou, Q., Zhang, W., Fu, Y. and Huang, H.** (2002). *ASYMMETRIC LEAVES1*, an *Arabidopsis* gene that is involved in the control of cell differentiation in leaves. *Planta* **214**, 694-702.
- Takayama, S., Shiba, H., Iwano, M., Shimosato, H., Che, F.-S., Kai, N., Watanabe, M., Suzuki, G., Hinata, K. and Isogai, A.** (2000). The pollen determinant of self-incompatibility in *Brassica campestris*. *Proc. Natl. Acad. Sci. USA* **97**, 1920-1925.
- Thompson, J.D., Higgins, D.G. and Gibson, T.J.** (1994). CLUSTAL W: improving the sensitivity of progressive multiple sequence alignment through sequence weighting, positions-specific gap penalties and weight matrix choice. *Nucl. Acid. Res.* **22**, 4673-4680.
- Tsuge, T., Tsukaya, H. and Uchimiya, H.** (1996). Two independent and polarized processes of cell elongation regulate leaf blade expansion in *Arabidopsis thaliana* (L.) Heynh. *Development* **122**, 1589-1600.
- Tsukaya, H.** (2002). Interpretation of mutants in leaf morphology: genetic evidence for a compensatory system in leaf morphogenesis that provides a new link between cell and organismal theories. *Int. Rev. Cytol.* **217**, 1-39.
- Tsukaya, H.** (2003). Organ shape and size: a lesson from studies of leaf morphogenesis. *Curr. Opin. Plant Biol.* **6**, 57-62.
- Tsukaya, H., Kozuka, T. and Kim, G.-T.** (2002). Genetic control of petiole length in *Arabidopsis thaliana*. *Plant Cell Physiol.* **43**, 1221-1228.
- Ullah, H., Chen, J.-G., Young, J.C., Im, K.-H., Sussman, M.R. and Jones, A.M.** (2001). Modulation of cell proliferation by heterotrimeric G protein in *Arabidopsis*. *Science* **292**, 2066-2069.
- Wang, H., Qi, Q., Schorr, P., Cutler, A.J., Crosby, W.L. and Fowke, L.C.** (1998). ICK1, a cyclin-

dependent protein kinase inhibitor from *Arabidopsis thaliana* interacts with both Cdc2a and CycD3, and its expression is induced by abscisic acid. *Plant J.* **15**, 501-510.

Wang, H., Zhou, Y., Gilmer, S., Whitwill, S. and Fowke, L.C. (2000). Expression of the plant cyclin-dependent kinase inhibitor ICK1 affects cell division, plant growth and morphology. *Plant J.* **24**, 613-623.

Weigel, D., Ahn, J.H., Blazquez, M.A., Borevitz, J.O., Christensen, S.K., Fankhauser, C., Ferrandiz, C., Kardailsky, I., Malancharuvil, E.J., Neff, M.M., Nguyen, J.T., Sato, S., Wang, Z.Y., Xia, Y., Dixon, R.A., Harrison, M.J., Lamb, C.J., Yanofsky, M.F. and Chory, J. (2000). Activation tagging in *Arabidopsis*. *Plant Physiol.* **122**, 1003-1013.

Wen, J., Lease, K.A. and Walker, J.C. (2004). DVL, a novel class of small polypeptides: overexpression alters *Arabidopsis* development. *Plant J.* **37**, 668-677.

Wilson, K., Long, D., Swinburne, J., and Coupland, G. (1996). A Dissociation insertion causes a semidominant mutation that increases expression of TINY, an *Arabidopsis* gene related to APETALA2. *Plant Cell* **8**, 659-671.

Yang, W.-C., Katinakis, P., Hendriks, P., Smolders, A., de Vries, F., Spee, J., van Kammen, A., Bisseling, T. and Franssen, H. (1993). Characterization of *GmENOD40*, a gene showing novel patterns of cell specific expression during soybean nodule development. *Plant J.* **3**, 573-585.

Yano, S. and Terashima, I. (2001) Separate localization of light signal perception for sun or shade type chloroplast and palisade tissue differentiation in *Chenopodium album*. *Plant Cell Physiol.* **42**, 1303-1310

Zhao, D., Yang, M., Solava, J. and Ma, H. (1999). The *ASK1* gene regulates development and interacts with the *UFO* gene to control floral organ identity in *Arabidopsis*. *Dev. Genet.* **25**, 209-223.

